united nations
educational, scientific
and cultural
organization

international atomic
energy agency

the
abdus salam
international centre for theoretical physics

SMR/1220-35

Workshop on

Nuclear Reaction Data and Nuclear Reactors: Physics, Design and Safety

13 March - 14 April 2000

Miramare - Trieste, Italy

Measurements of microscopic high energy data

Sylvie LERAY
Centre d'Etudes Nucleaires de Saclay
Gif-sur-Yvette, France

Measurements of microscopic high energy data

- **Neutrons**
  - ➥ multiplicity distributions
  - ➥ double-differential cross-sections
- **Charged particles**
  - ➥ multiplicities
  - ➥ differential cross-sections
- **Residual nuclides**
  - ➥ spectroscopy
  - ➥ in-line mass-spectrometry
  - ➥ inverse kinematics
- **Coincidence measurements**
  - ➥ light charged particles, fission fragments and low energy neutrons
    - ⇨ deeper insight of the reaction mechanisms

Neutron multiplicity distribution measurements with liquid scintillator neutron balls

collaboration HMI-Berlin, GANIL, Varsaw

Detection of low energy neutrons (below 20 MeV)

⇒ **sensitivity to the amount of excitation energy at the end of the cascade stage**

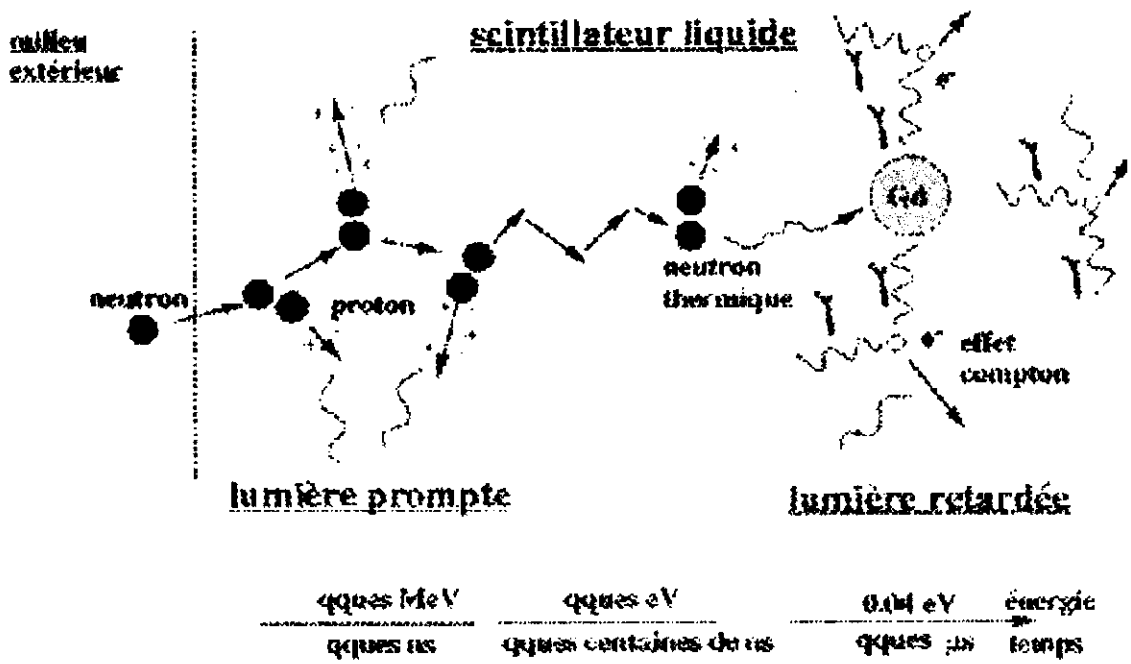

INC calculation from Cugnon (NP A462 (198
+ GEMINI (NP A483 (1988)) evaporation
corrected for detection efficiency

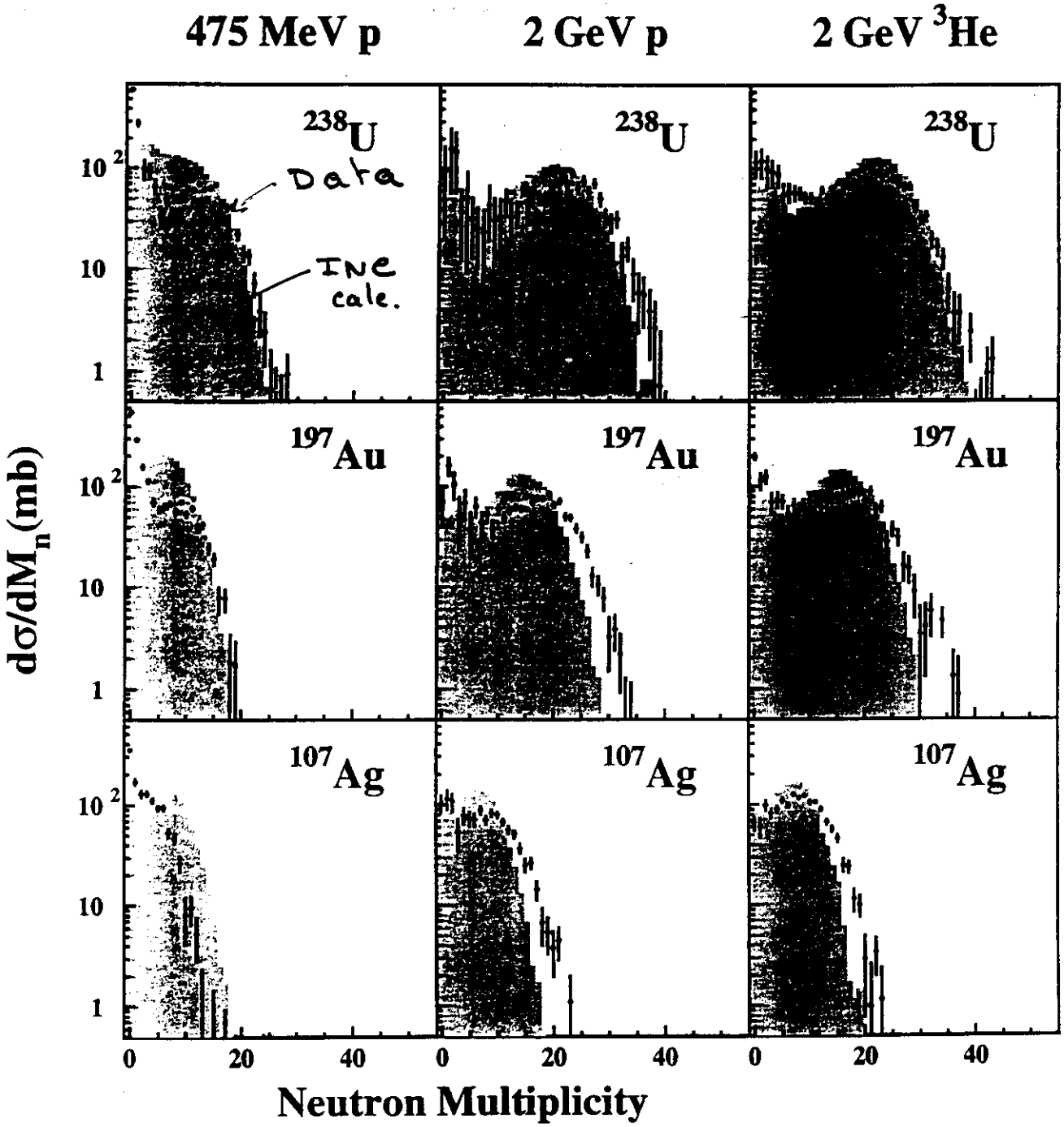

Phys. Rev. C May 98

X. LEDOUX et al Fig. 7

Neutron measurements

Angle and energy spectrum measurements

• **Measurement of neutron production double-differential cross-sections at SATURNE**

Measurement method:

- from 3 MeV to 400 MeV: time of flight between tagged incident proton and a neutron scintillator

- from 100 MeV to incident energy: $n-p$ conversion in a H_{2liq} target and a magnetic spectrometer

- Use of quasi-monokinetic neutron beams (break-up $d+Be$) for efficiency determination

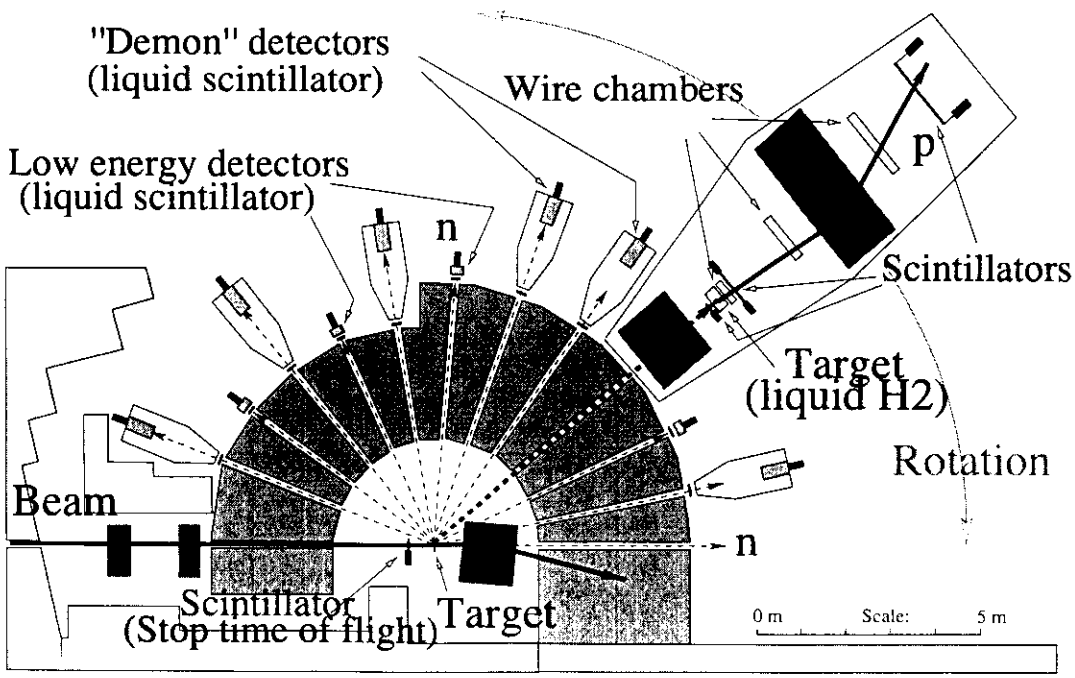

Experimental setup

Low Energy Detection

⇒ from 4 to 400 MeV DEMON detectors

⇒ from 2 to 16 MeV DENSE detectors

Determination des efficacités en énergie :

- on Bruyères-le-Châtel Tandem from 2 to $16 MeV$ using $^{3}H(p,n)^{3}He$ and $^{3}H(d,n)^{4}He$ reactions

- at Uppsala from 30 to $120 MeV$ by associated particle method

- at Saturne from 150 to $800 MeV$ through $d+Be$ cross-section

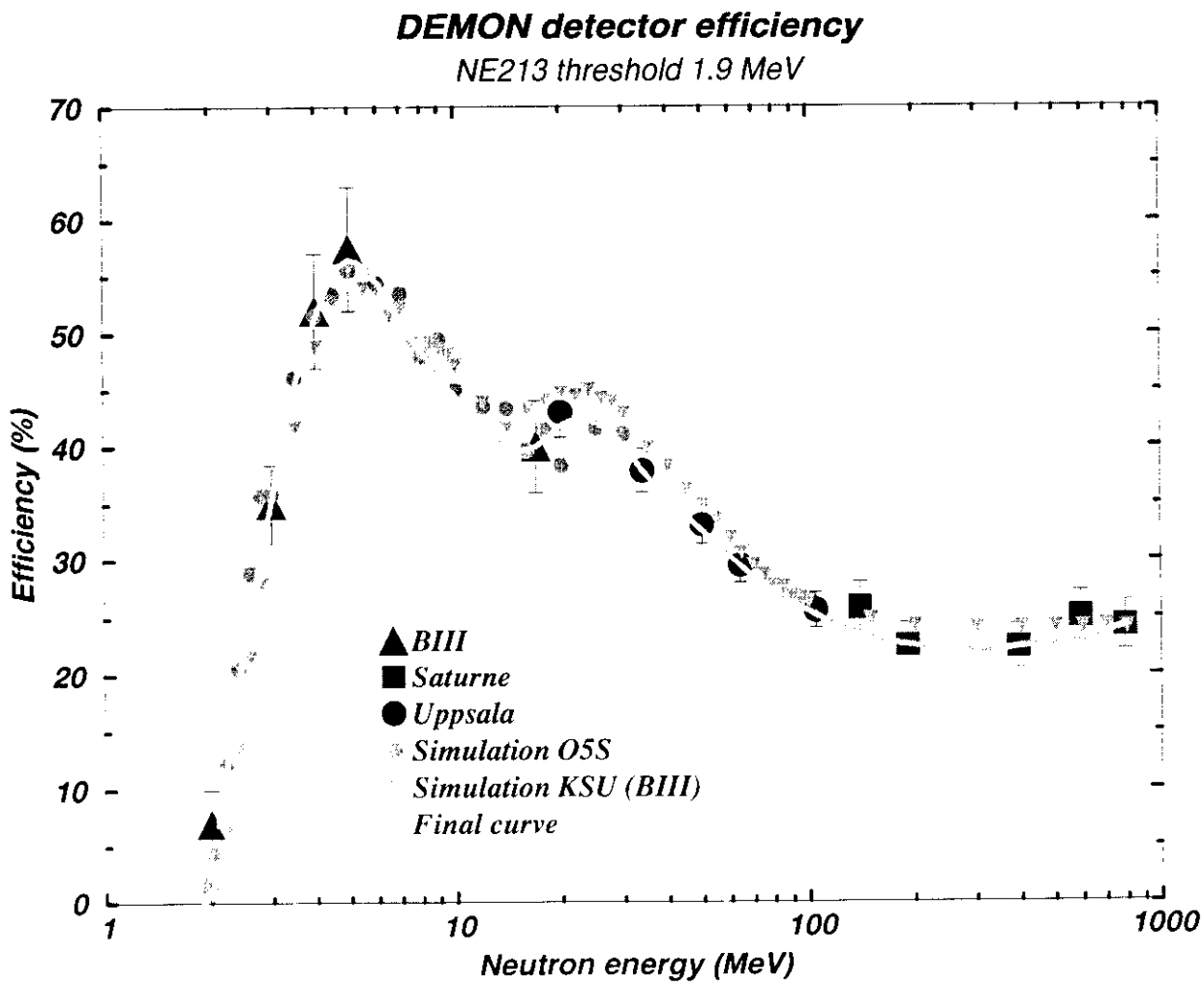

• Measurement of the spectrometer response function:

obtained with quasi-monokinetic neutrons produced in reaction:

- $d + Be$ up to $1.15\,GeV/A$
- $^3He + Be$ from $1.15\,GeV/A$ to $1.6\,GeV/A$

⇒ Détermination of the absolute neutron flux:

$\sigma_{elastic}(n,p)$ limited to $[0, 3°]$ aperture where acceptance is 100%

⇒ measurement of the response function to quasi-monokinetic neutrons:

measurement with total acceptance

⇒ Fit of the response at different energies: 4 gaussians the parameters of which are a function of energy

⇒ Déconvolution

Neutron measurements at SATURNE

⇒ Thin target

- Measurement of energy-distributions at various angles from 0° to 160°
- Protons and deuterons between 0.8 and 1.6 GeV on Al, Fe, Zr, W, Pb, Th

⇒ Thick targets

- Measurement at various angles on targets of different diameters as a function of position in the target
- Protons and deuterons between 0.8 and 1.6 GeV on Al, Fe, W, Pb

Neutron production double-differential cross-sections

collaboration CEA/DSM, CEA/DAM, IN2P3

⇒ Comparison of two different INC models inside the TIERCE HETC code

(same Dresner-Atchison evaporation-fission code)

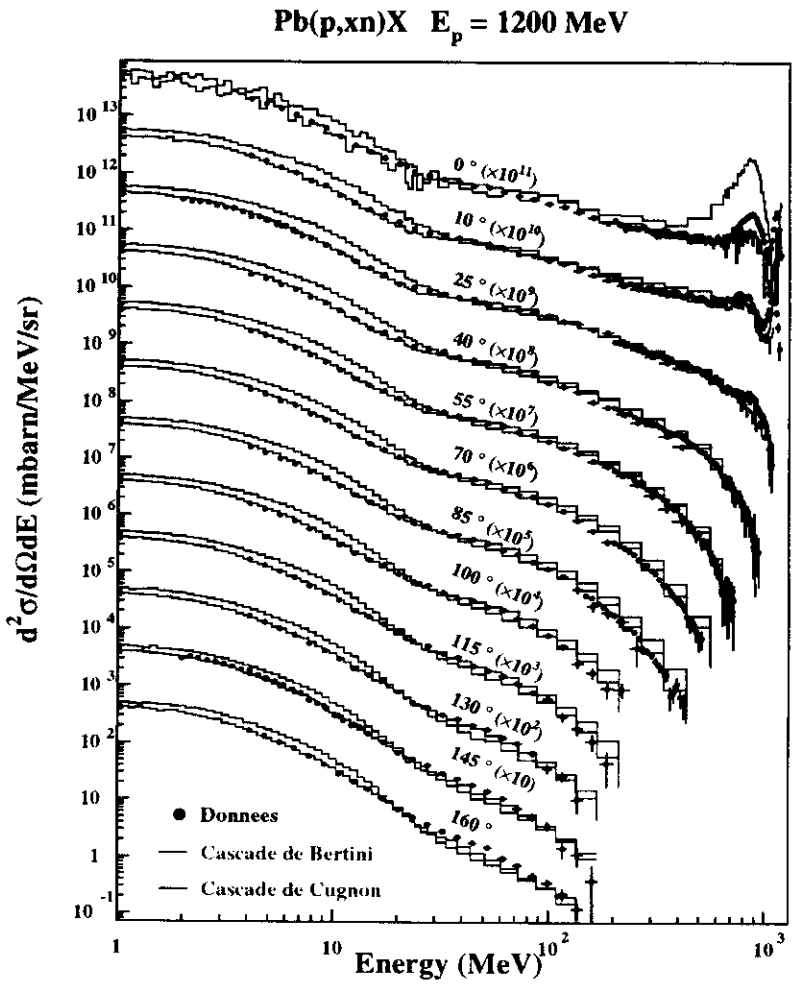

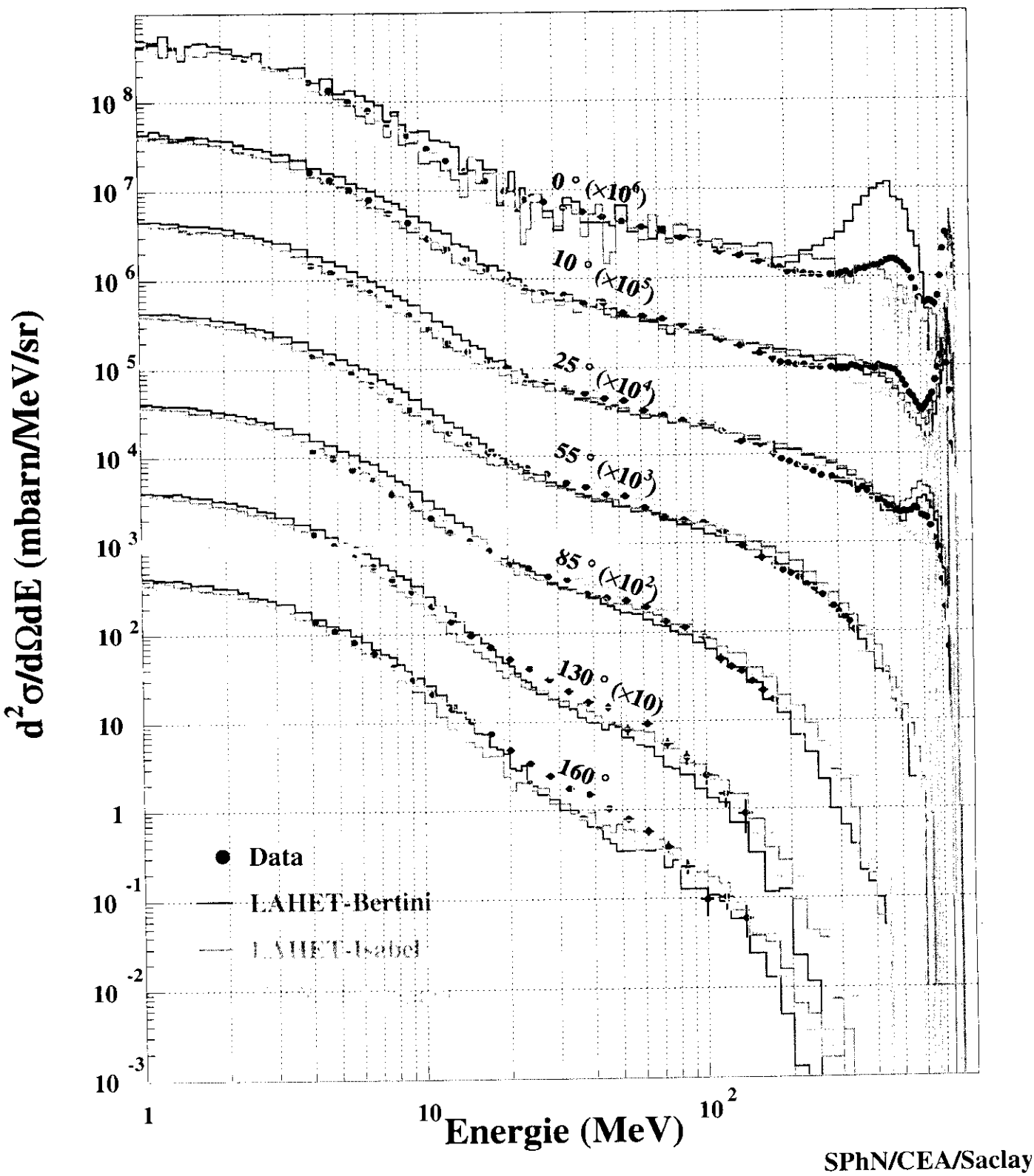
Pb(p,xn)X 800 MeV (Evapo Dresner)
d²σ/dΩdE (mbarn/MeV/sr)
Energie (MeV)
0 ° (×10⁶)
10 ° (×10⁵)
25 ° (×10⁴)
55 ° (×10³)
85 ° (×10²)
130 ° (×10)
160 °
Data
LAHET-Bertini
LAHET-Isabel
SPhN/CEA/Saclay

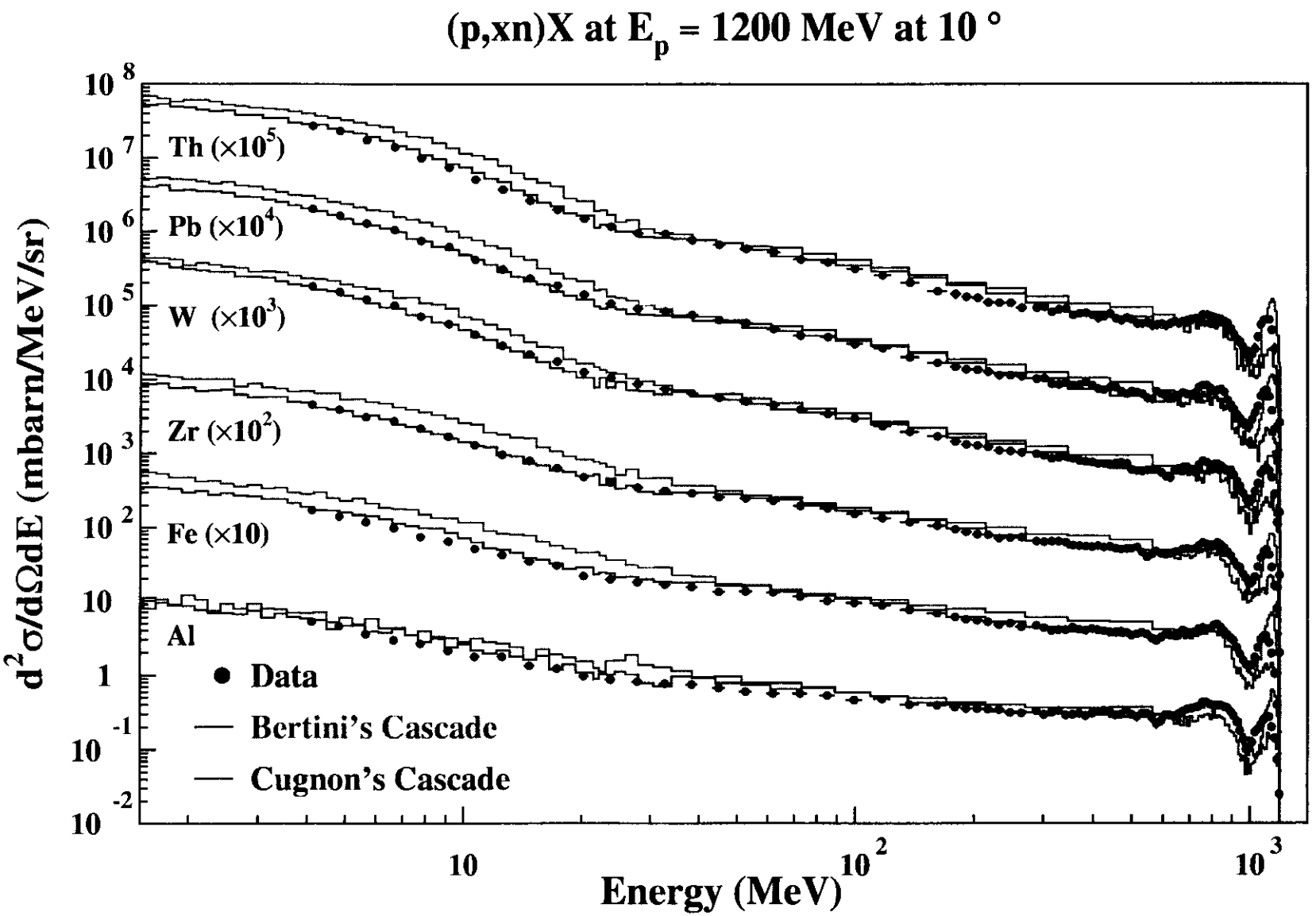
(p,xn)X at E_p = 1200 MeV at 10 °
d²σ/dΩdE (mbarn/MeV/sr)
Th (×10⁵)
Pb (×10⁴)
W (×10³)
Zr (×10²)
Fe (×10)
Al
Data
Bertini's Cascade
Cugnon's Cascade
Energy (MeV)

표 1.6

Per reaction total neutron multiplicities

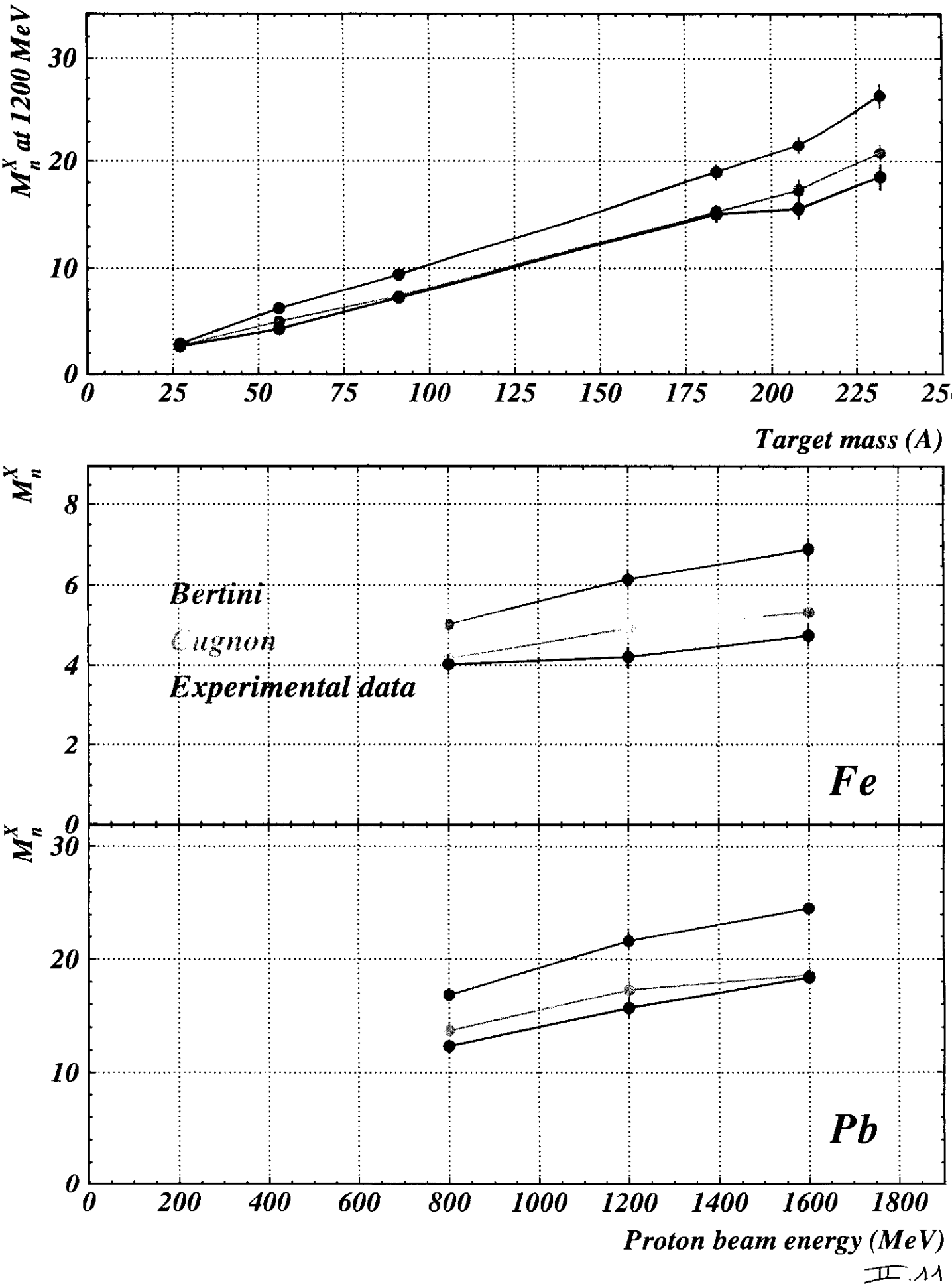

III.11

Per reaction averaged neutron multiplicities and energy carried out by the emitted neutrons obtained by integration of the double-differential cross-sections over the angular distribution and compared with calculations using [illegible] with Cugnon[2] or Bertini[3] INC model and [illegible] for a 2cm Pb target.

Energy	$M_n^{[illegible]}$	M_n^{Cug}	M_n^{Tie}	M_n^{Lah}	$E \times M_n^{[illegible]}$	$E \times M_n^{Cug}$	$E \times M_n^{Tie}$	$E \times M_n^{Lah}$
[illegible]								
0 - 2 MeV		4.9	6.1	5.6		4.8	6.2	5.7
2 - 20 MeV	6.5 ± 1.0	6.9	9.5	8.6	38. ± 4.	42.	55.	50.
20 - E_{max}	1.9 ± 0.2	2.2	1.8	1.8	200. ± 20.	211.	203.	202.
TOTAL		14.0	17.4	16.0		258.	264.	258.
[illegible]								
0 - 2 MeV		5.8	6.9	6.3		5.8	7.0	6.5
2 - 20 MeV	8.3 ± 1.0	8.9	12.4	11.4	52. ± 6.	54.	78.	71.
20 - E_{max}	2.7 ± 0.3	2.8	2.4	2.4	310. ± 31.	309.	294.	299.
TOTAL		17.4	21.7	20.2		369.	379.	377.
[illegible]								
0 - 2 MeV		6.0	7.4	6.8		6.0	7.5	7.0
2 - 20 MeV	10.1 ± 1.4	10.0	14.7	13.6	65. ± 8.	61.	97.	90.
20 - E_{max}	3.4 ± 0.4	3.1	3.1	3.1	410. ± 40.	422.	373.	389.
TOTAL		19.1	25.2	23.5		489.	478.	486.

2) J.Cugnon, Nucl. Phys. A462 (1987) 751; J.Cugnon *et al.* Nucl. Phys. A620 (1997) 475.

4) R.E.Prael *et al.*, *LAHET*^{TM} Code System, Report LA-UR-89-3014, LANL 1989.

Measurements of hydrogen and helium production

Thin targets

collaboration NESSI (Berlin, Jülich, GANIL)

Calculations with the Cugnon model

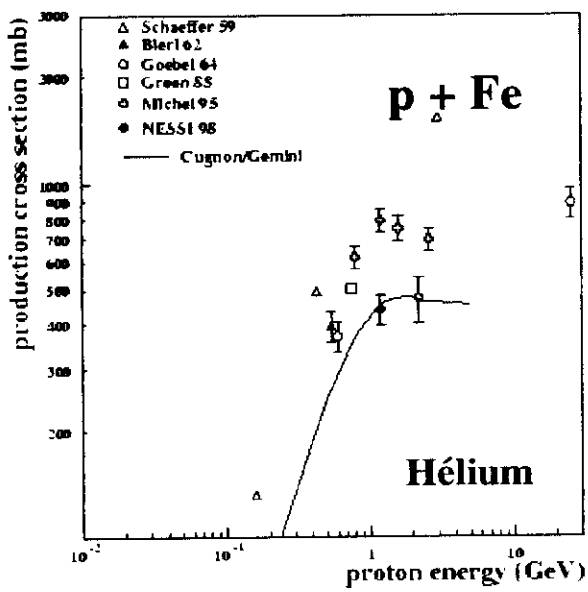

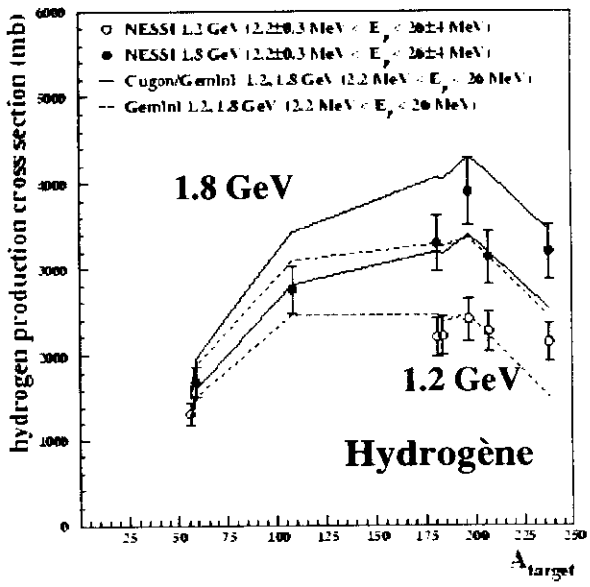

From Enke et al., 1998 Annual Report Bereich Festkörperphysik, HMI-Berlin

II . 13

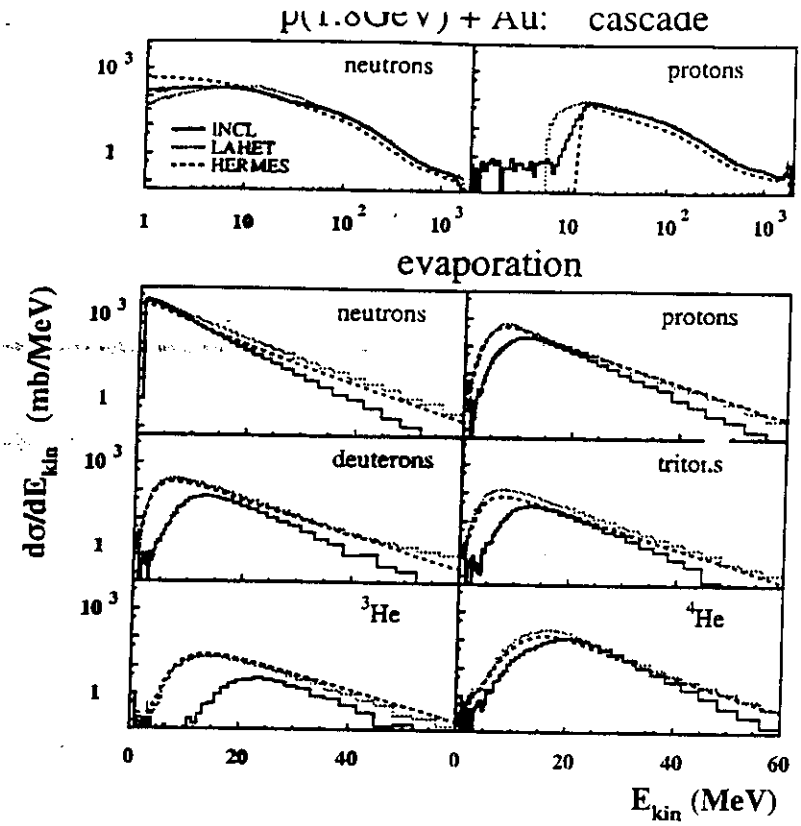

Fig. 15. Comparison of calculated particle energy spectra with the INCL (solid histogram) and LAHET-code (dotted histogram). The top two panels represent the nucleons emitted during the INC while the lower panels display the energy spectra of evaporated particles.

From Enke et al., NP A657 (1999) 317

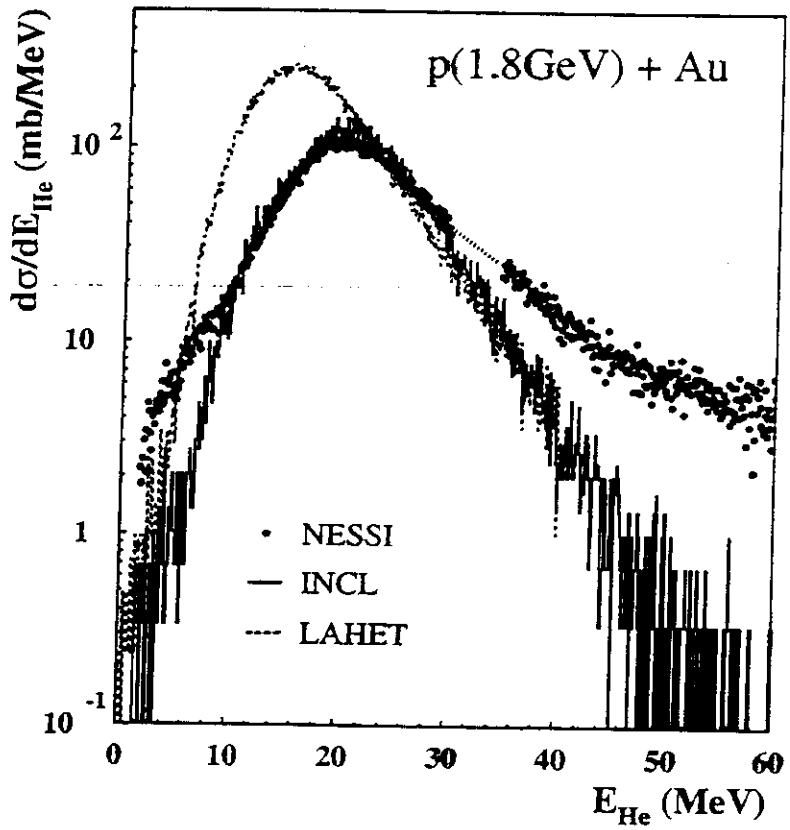

Fig. 16. Comparison of measured (solid circles) and calculated helium energy spectra with the INCL (solid histogram) and LAHET-code (dashed histogram). The experimental helium spectrum was integrated over $0 < \theta < 66^0$ and $114 < \theta < 180^0$, the Au target thickness was 8.7 mg/cm^2.

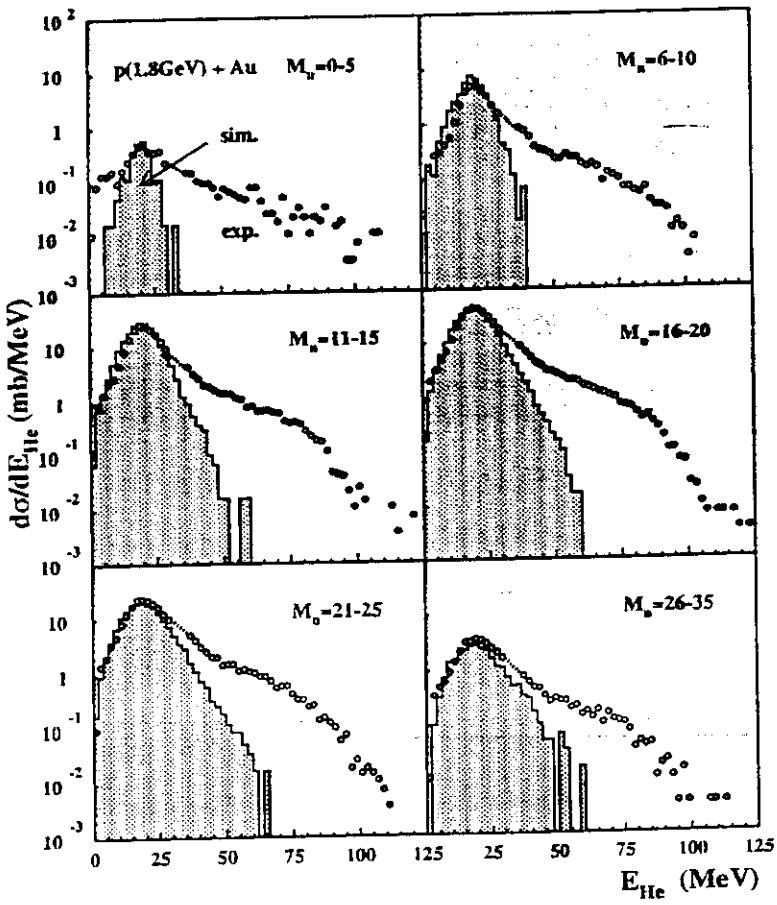

Fig. 9. Angle integrated He energy spectra (circles) as a function of measured neutron multiplicity for 1.8 GeV p + Au compared with INCL calculations.

From Enke et al., NP A657 (1999) 317

Residual nuclide production

γ-spectroscopy method

- production of nuclides on thin targets from a large variety of targets from 0.2 to 2 GeV on different accelerators [illegible], on W, Pb, U at SATURNE [illegible]

Mass-spectrometry method

- Measurement of ^{238}U and ^{232}Th isobaric production cross-sections at PSI [illegible]

Reverse kinematics method

- Measurement of complete isotopic distribution of spallation residues using reverse kinematics at GSI in Au, U and Pb + H_2 and D_2 reactions [illegible]

[redacted]

PE170, K.Sümmerer et al., Phys. Rev. C42 (1990) 2546

- **Radiochemical techniques to identify near-target residues**

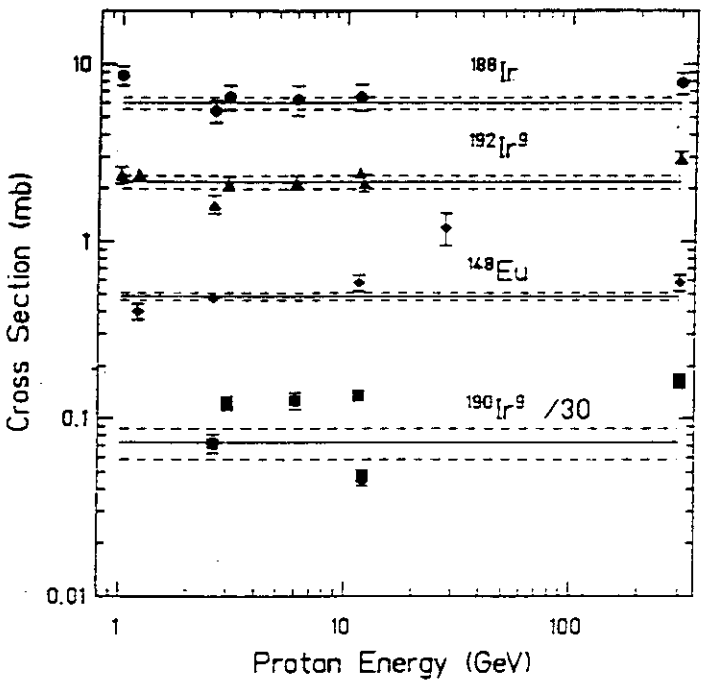

⇒ **Empirical parametrization of the mass and charge yields of spallation products**

⇒ **Target residue distribution becomes energy independent above a certain threshold**

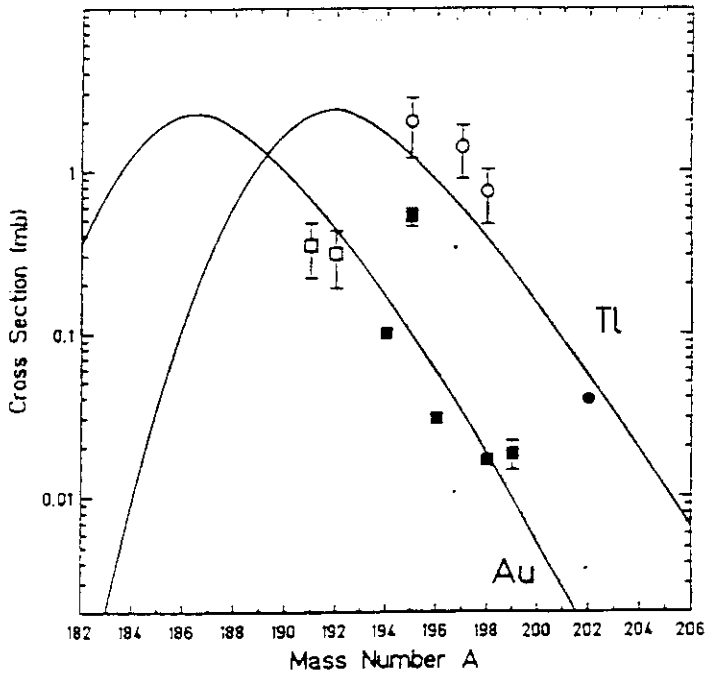

From R. Michel et al., NEA/OECD Intercomparison (1996)

Fig. 330: Au-197 (p, 3p3n) Ir-192

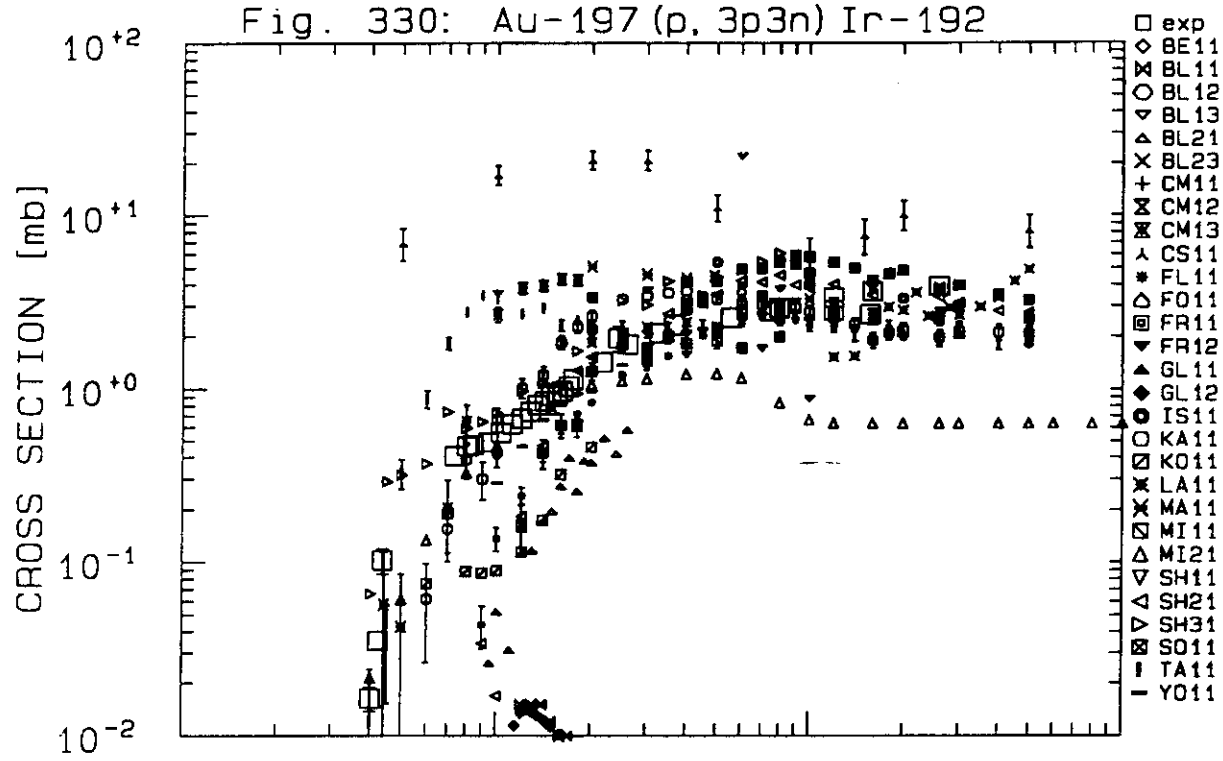

Fig. 331: Au-197 (p, 2p8n) Pt-188

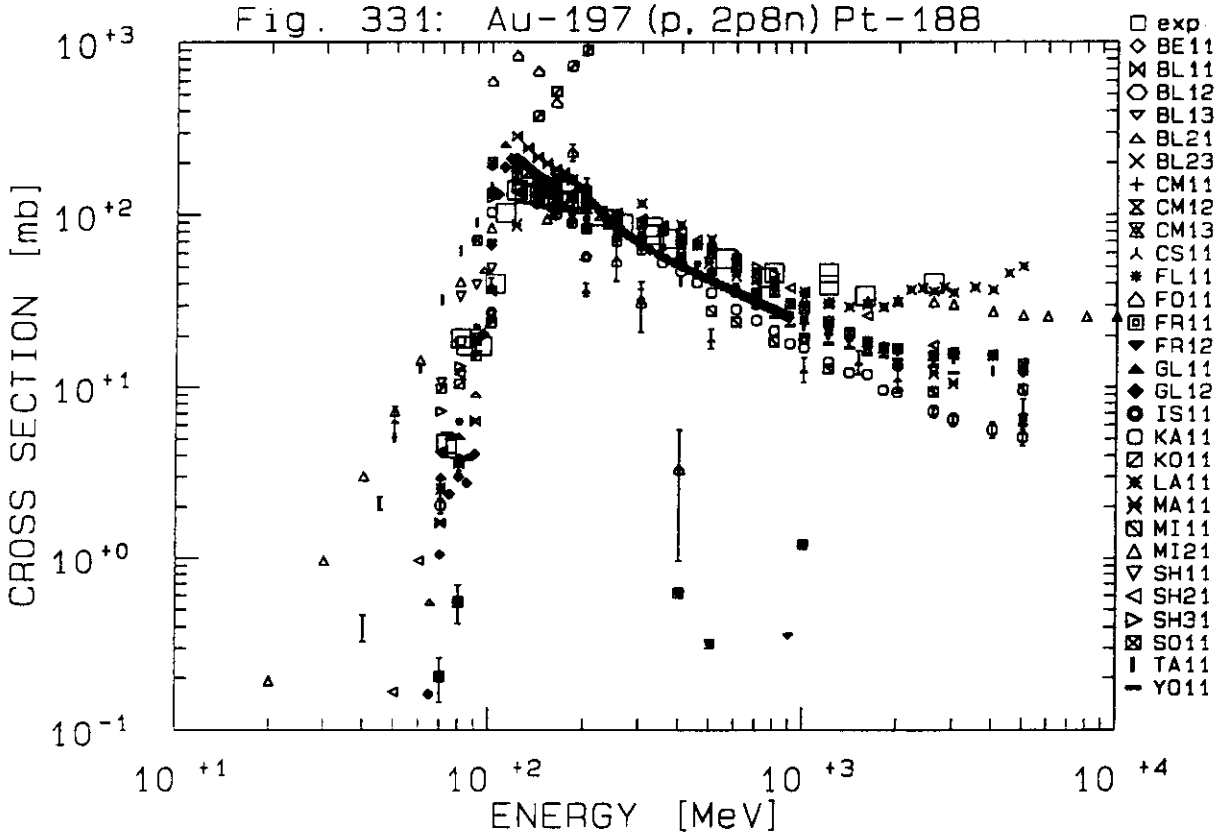

II.18

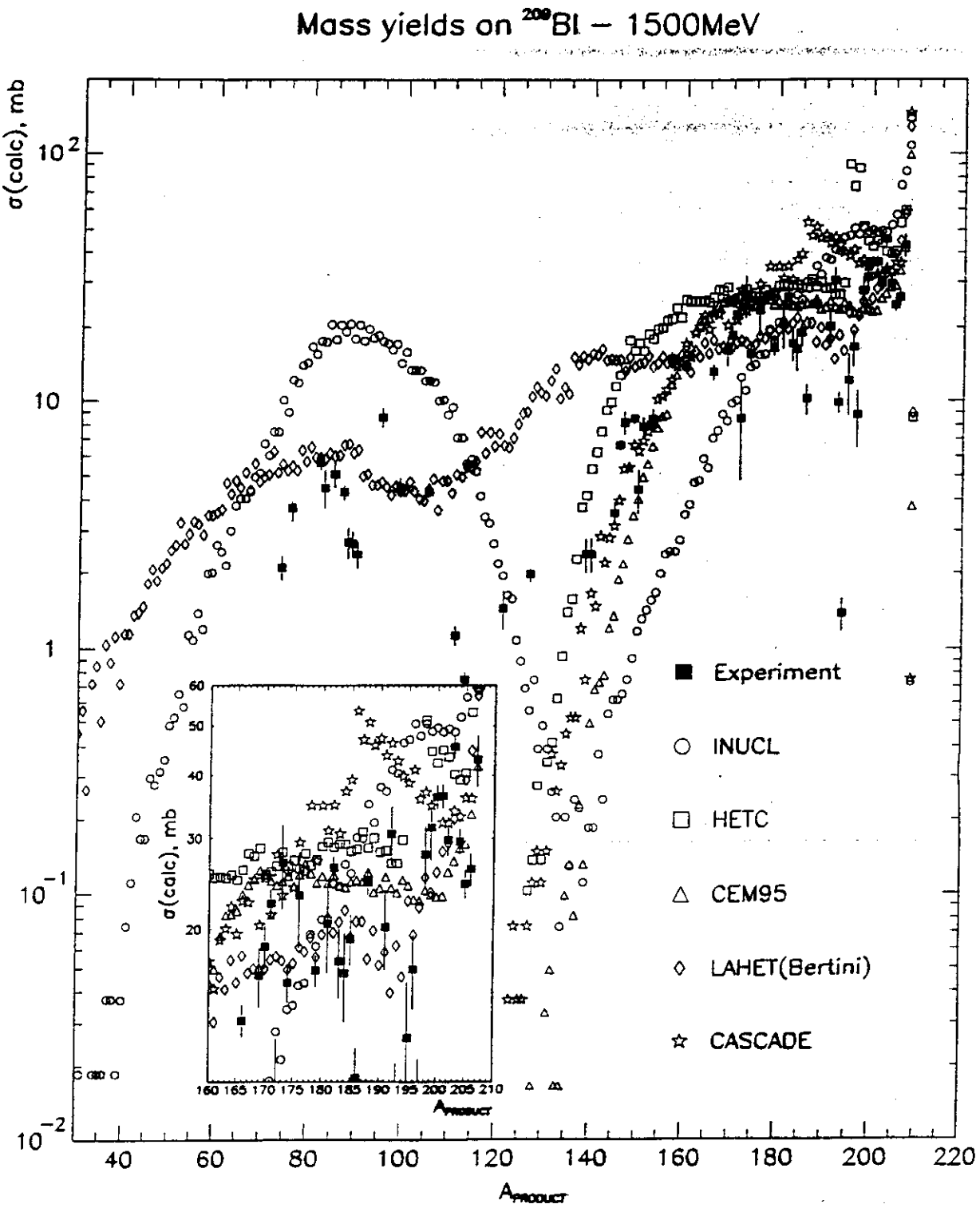

Fig. 10. Product mass distribution of the ^{209}Bi(p, x)-reaction for $E_p = 1500$ MeV proton.

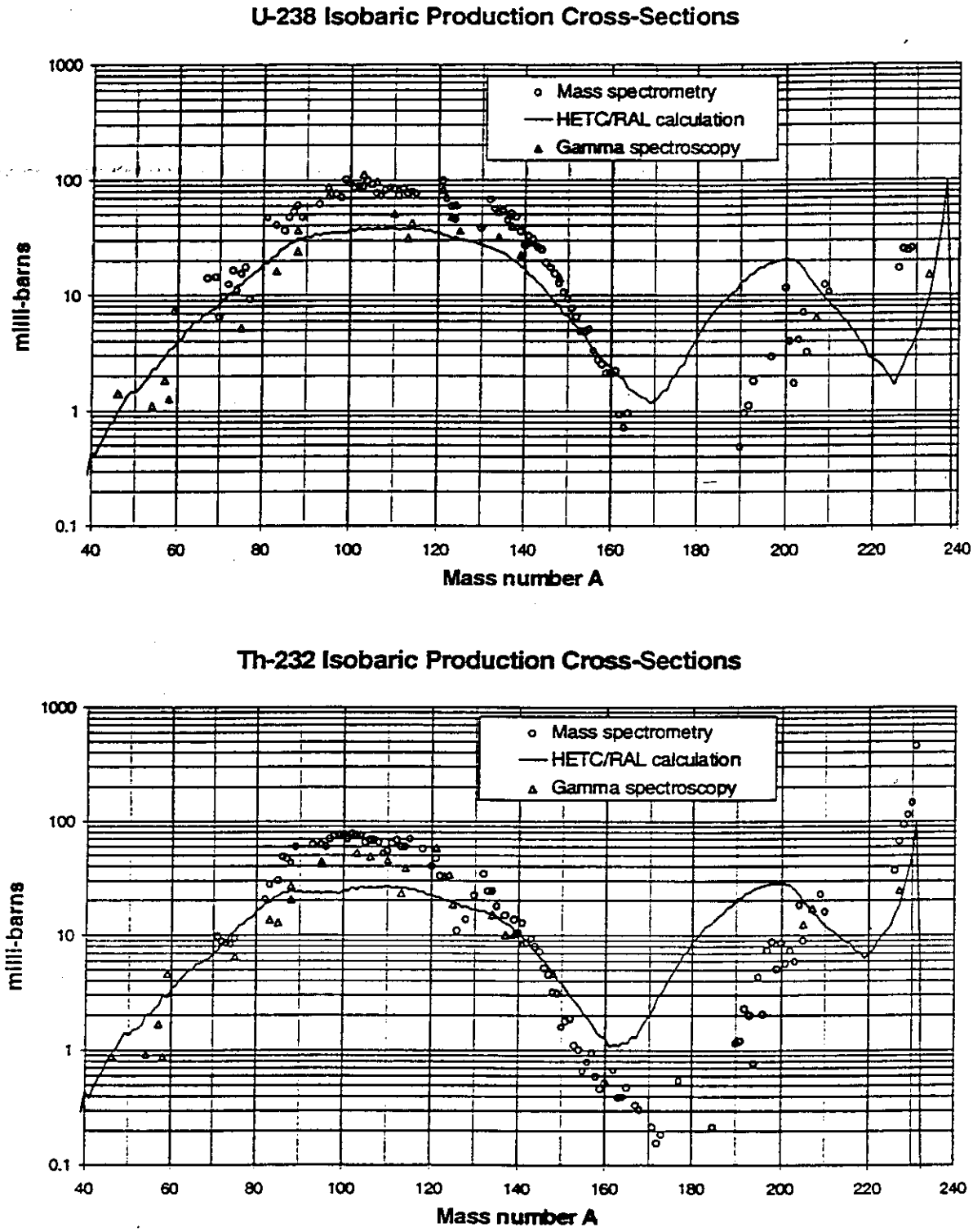

Fig.III-3[88]: Comparaison des sections efficaces de production isobarique du Th^{232} et de l'U^{238} déduites par spectrométrie de masse et spectrométrie gamma avec les valeurs calculées par HETC

From H.U. Wenger et al., proc. PHYSOR 96, vol. 4, M-73, Sept. 96, Mito, Japan

GSI Fragment Separator

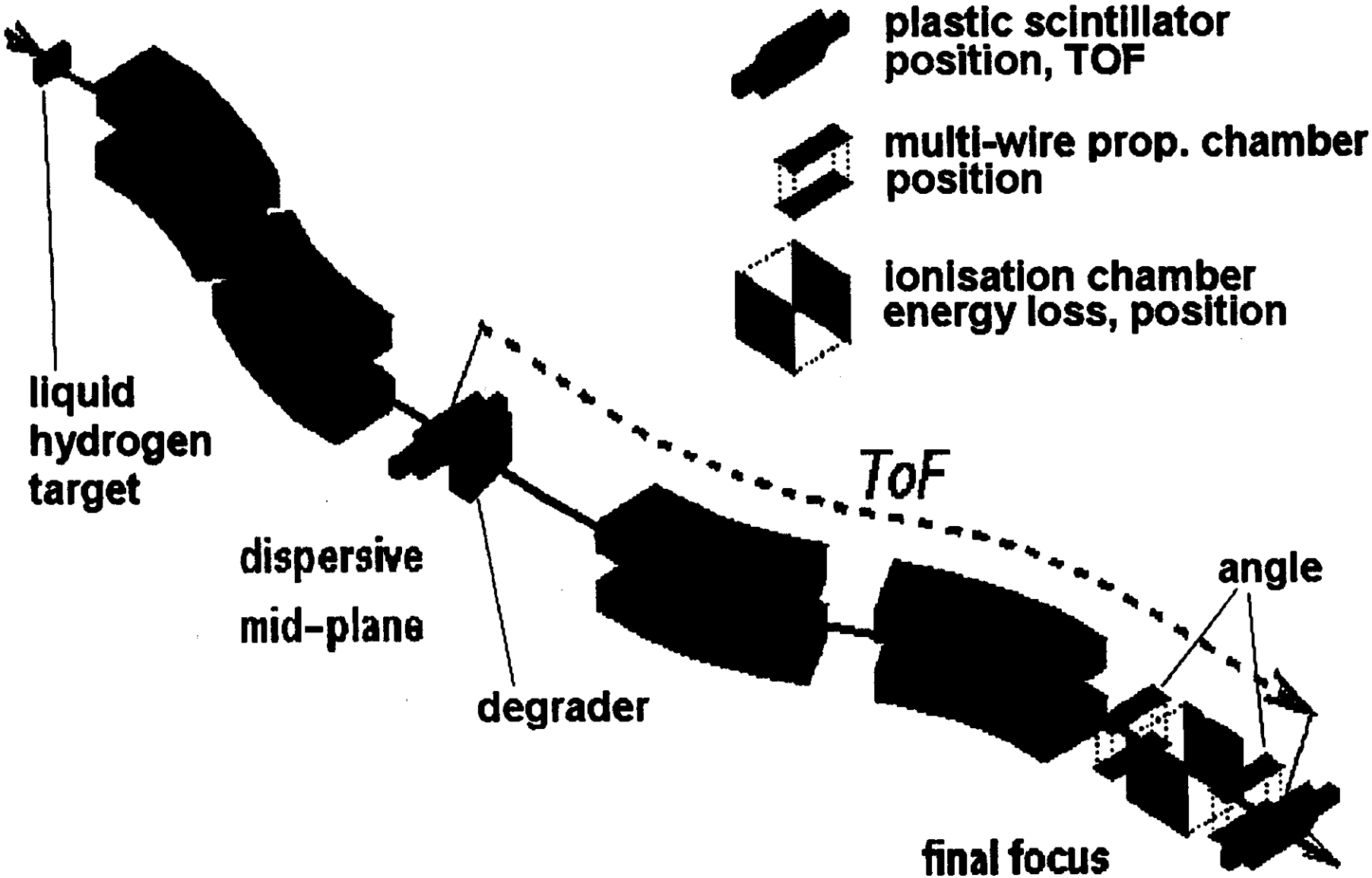

Isotopic Distributions 1 A GeV ^{208}Pb + p

Coll. GSI, DAPNIA/SPhN, IPN Orsay, Santiago Univ., CENBG Bordeaux

☆ Michel et al., to appear in NIM (2000)

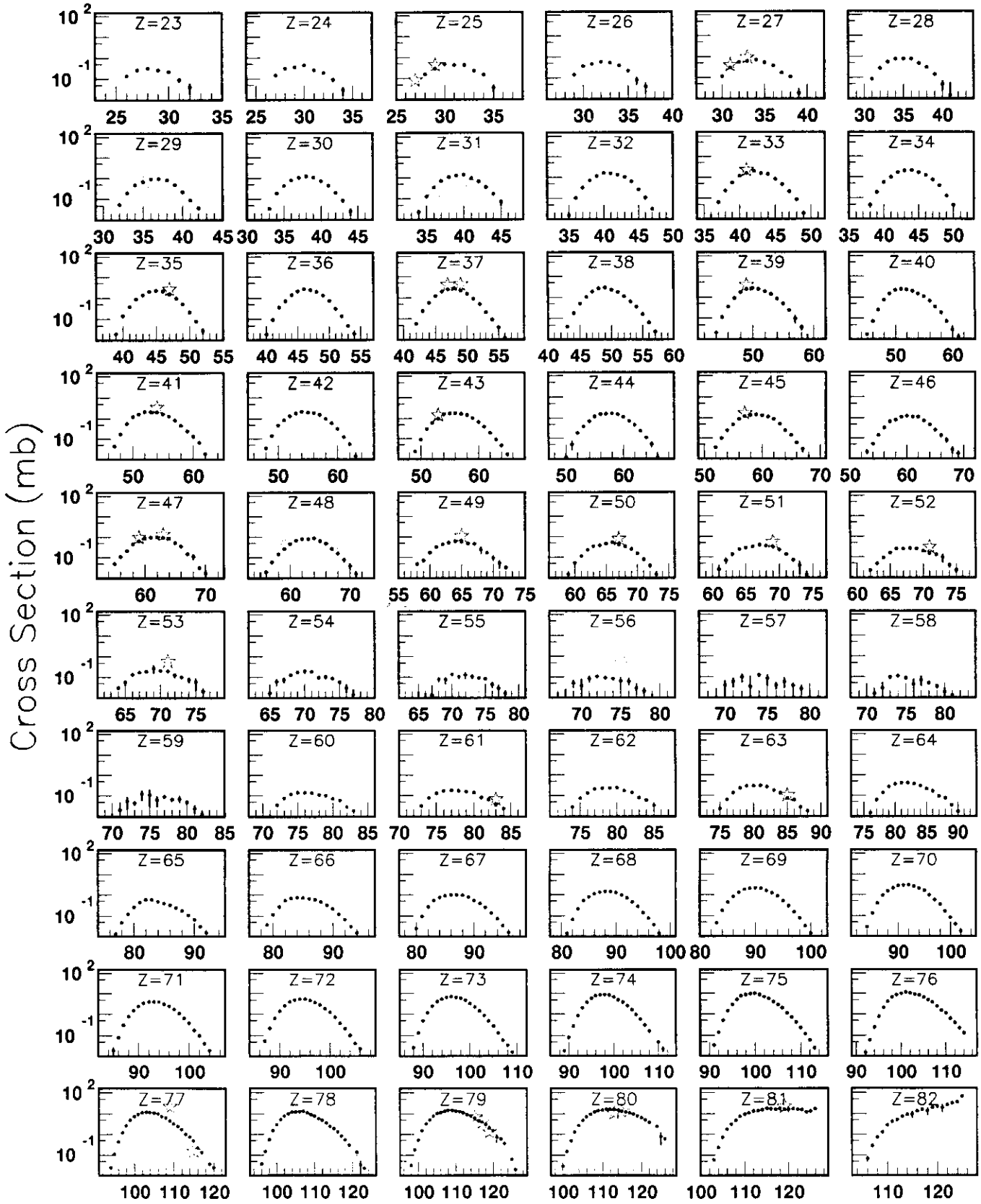

Wlazlo et al., submitted to PRL

Preprint DAPNIA/SPhN-00-10,

Comparison of INC Codes

Mass distributions

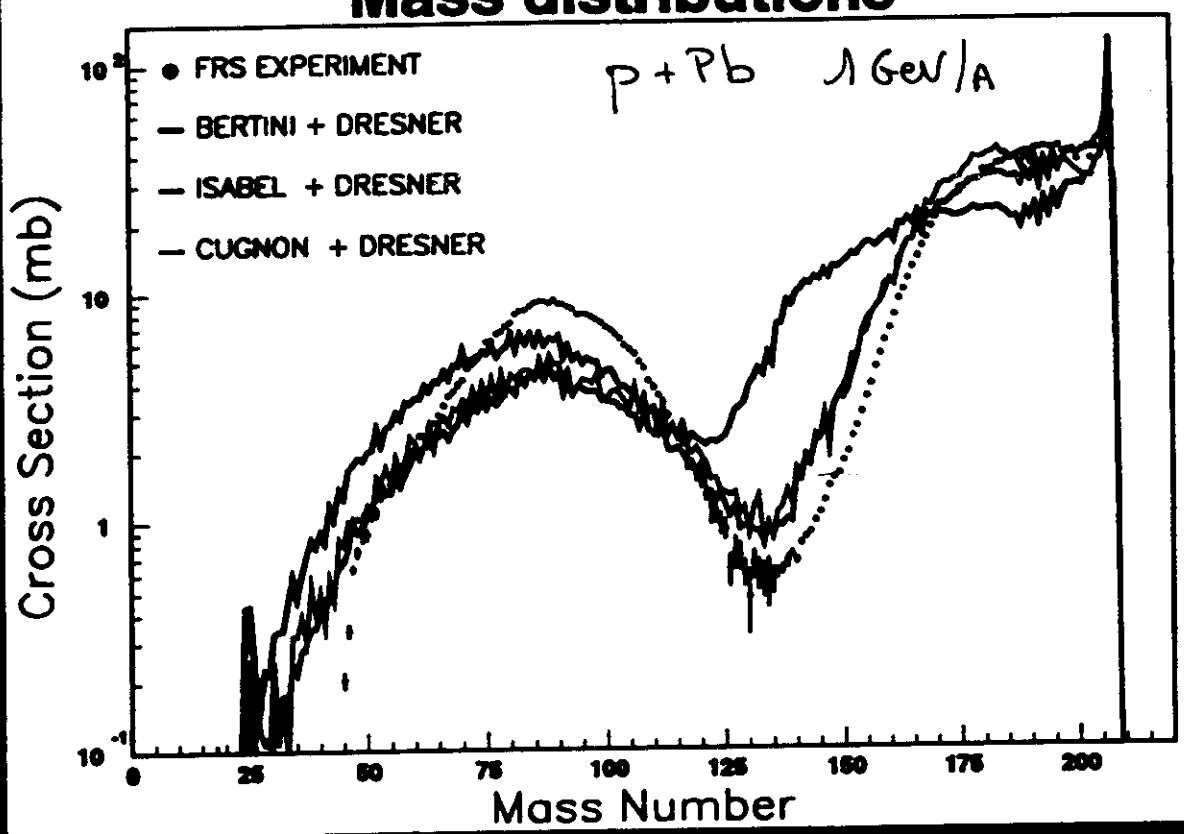

Isotopic distribution

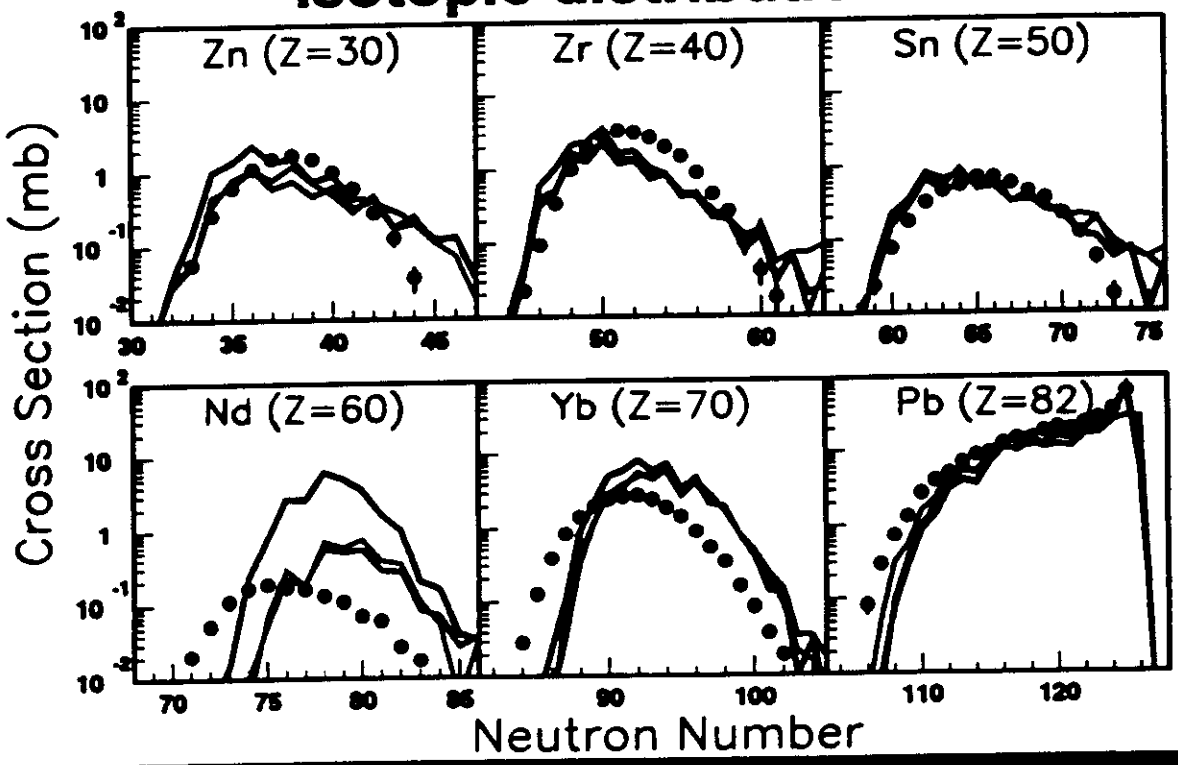

1 GeV Pb+p,cugnon_3 (trapeze vuillier, z OK) + KHS_V3, V=45MeV, t0/0.85

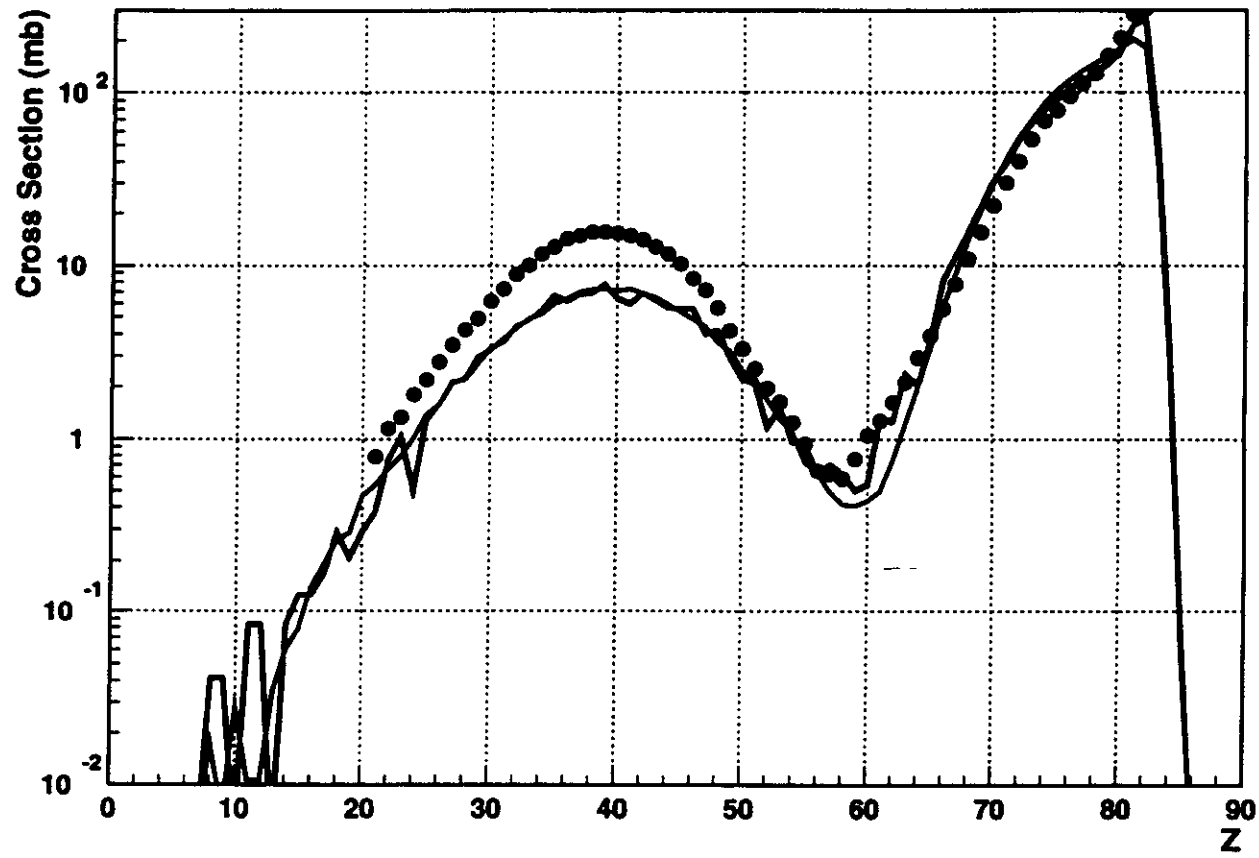

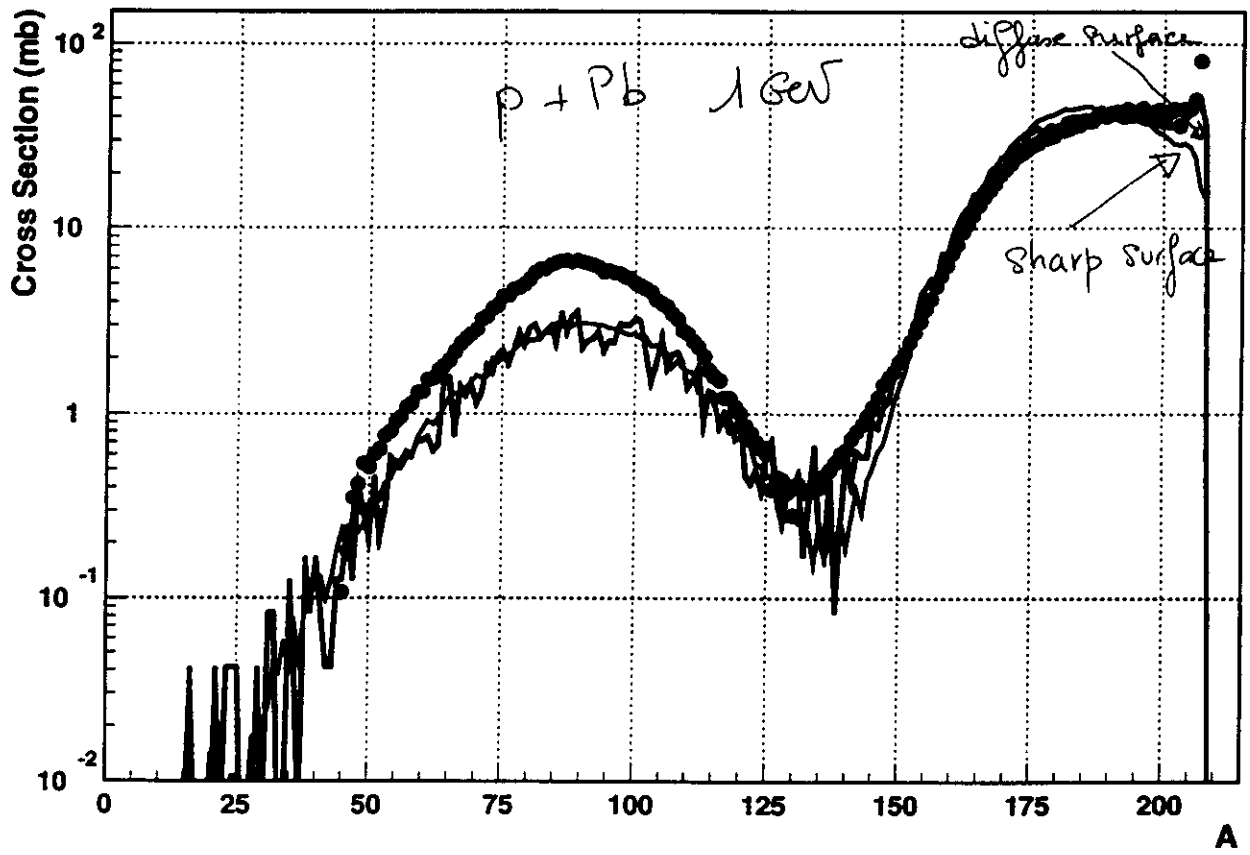

II.24

00/03/14 10.31

1 GeV Pb+p,cugnon_3 (trapeze vuillier, z OK) + KHS_V3, V=45MeV, t0/0.85

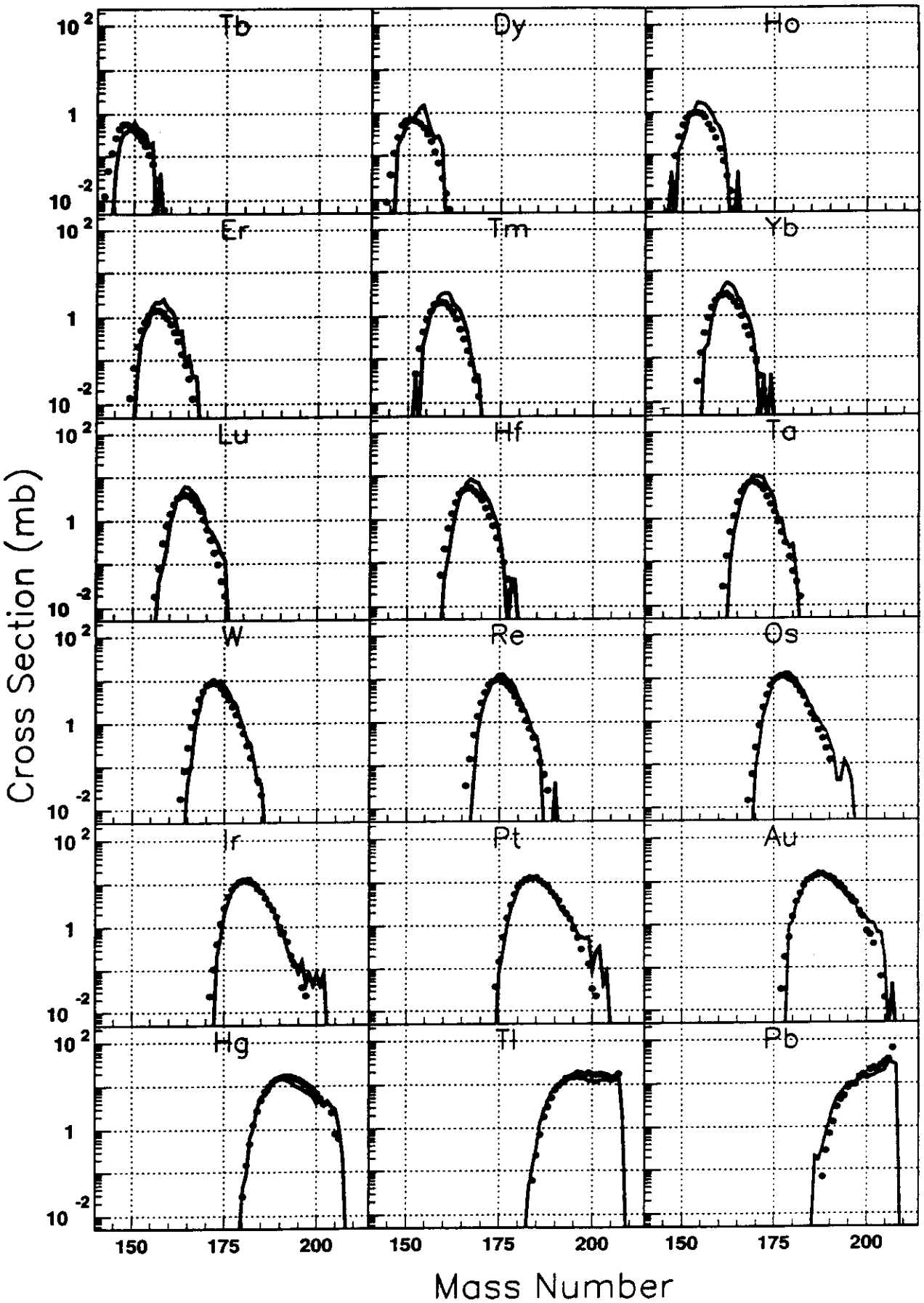

II.25

Important parameters in spallation source design

Neutron economy

⇒ choice of beam energy, nature

⇒ choice of target nature, geometry

Spatial distribution of neutron flux

⇒ optimisation of target shape

Shielding

⇒ minimisation of high energy neutrons

⇒ beam shape

Material problems

- energy deposition (target, window)

- activation (target, structures)

- DPA, gas production (window, structures)

- corrosion (liquid target)

⇒ choice of target nature

⇒ choice of window composition, thickness

⇒ choice of beam energy

Neutron production in thick targets

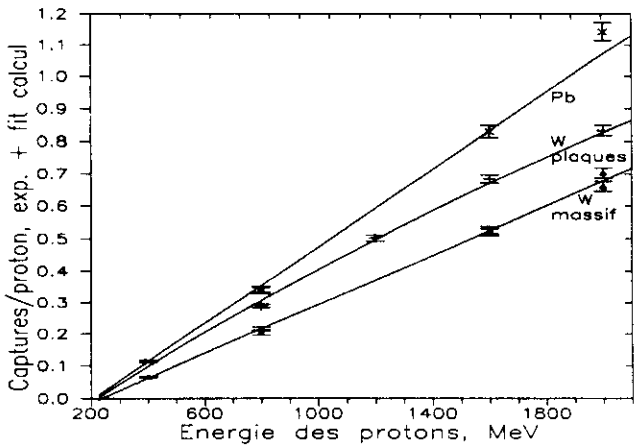

Data obtained by manganese bath technique compared with calculations performed with the code TIERCE from Bruyères-le-Châtel.

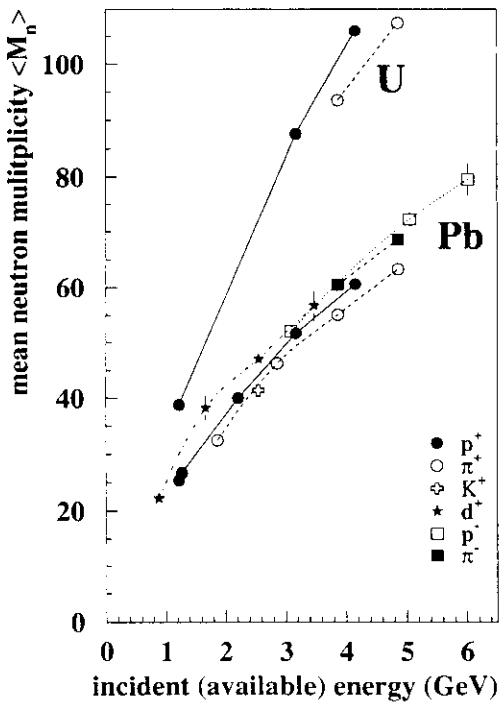

Mean neutron multiplicity for incident particles on 35 cm long 15 cm diameter Pb and 40 cm long 8 cm diameter depleted U targets.

Neutron multiplicity measurements

Thick target results

collaboration NESSI (Berlin, Jülich, GANIL)

Data : Target Pb, length 35cm, diameter 15cm

Calculation: HERMES (Jülich)

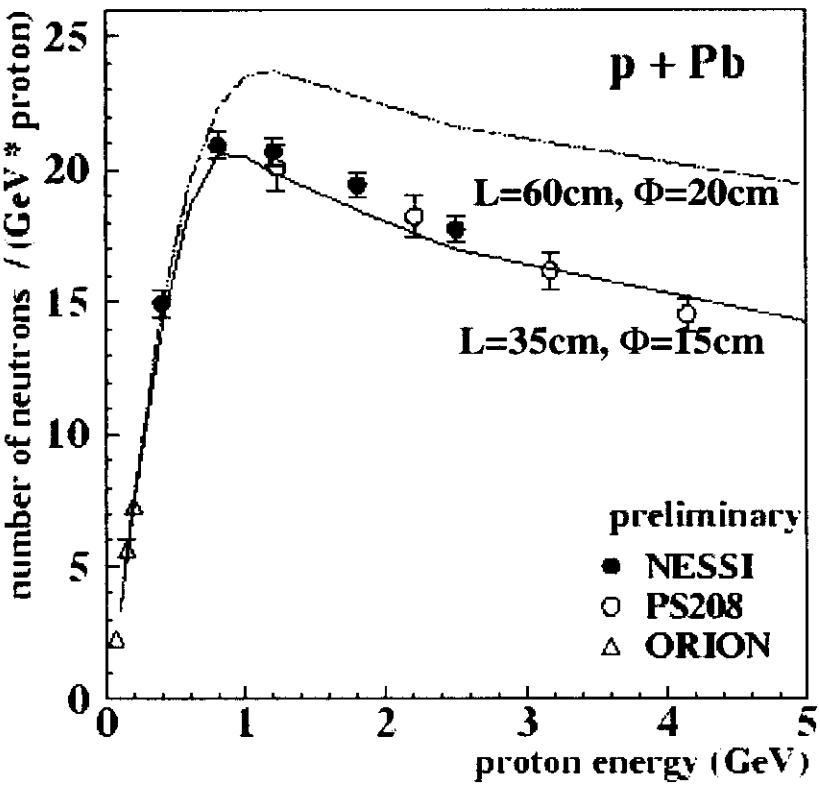

From Enke et al., 1998 Annual Report Bereich Festkörperphysik, HMI-Berlin

Energy dependence of neutron production

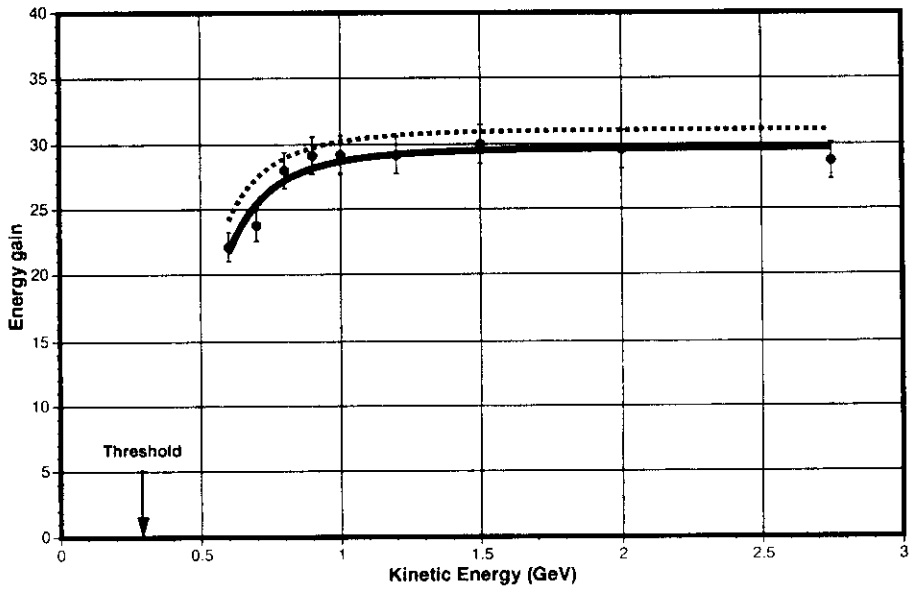

Energy gain of a cylindrical depleted U target surrounded by a sub-critical fuel assembly of natural U ı ›y water.

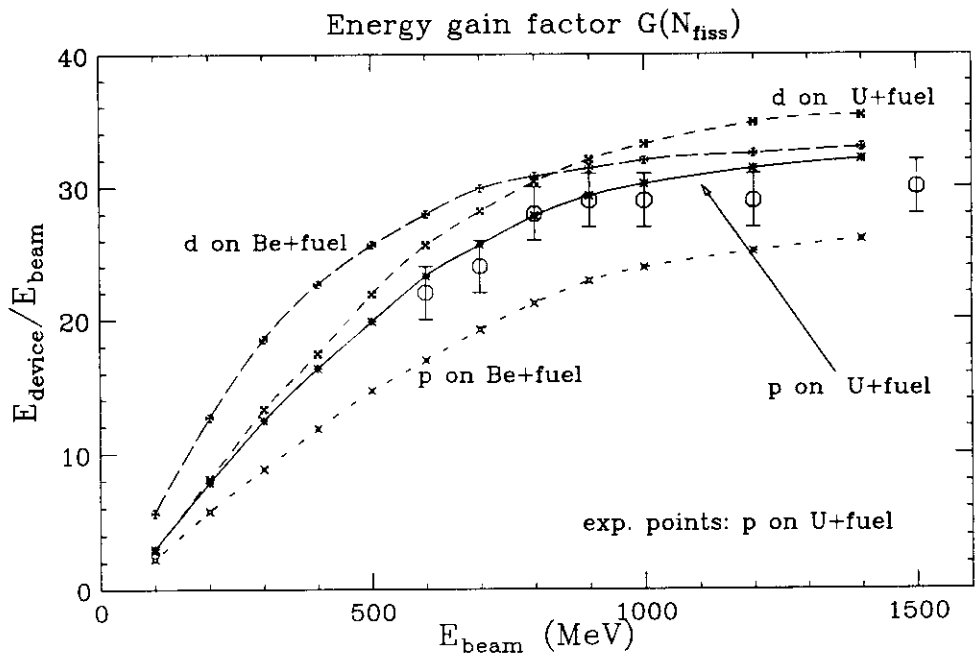

Idem compared with LAHET calculations for p and d beams on Be or U targets.

Shape optimisation of a spallation target

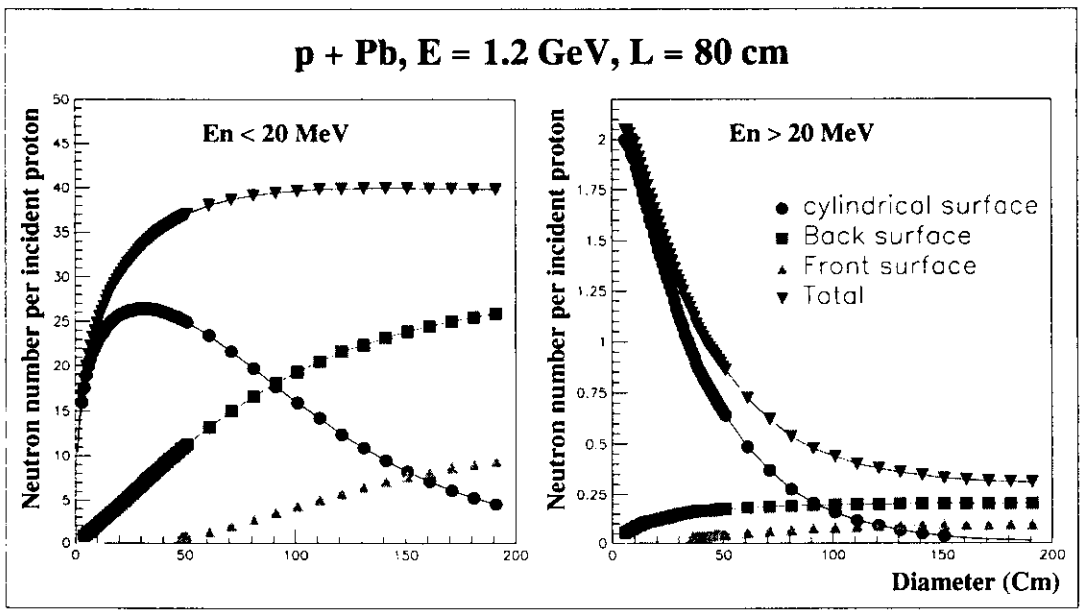

Number of low and high energy neutrons emitted through the different faces of a cylindrical lead target as a function of the target diameter.

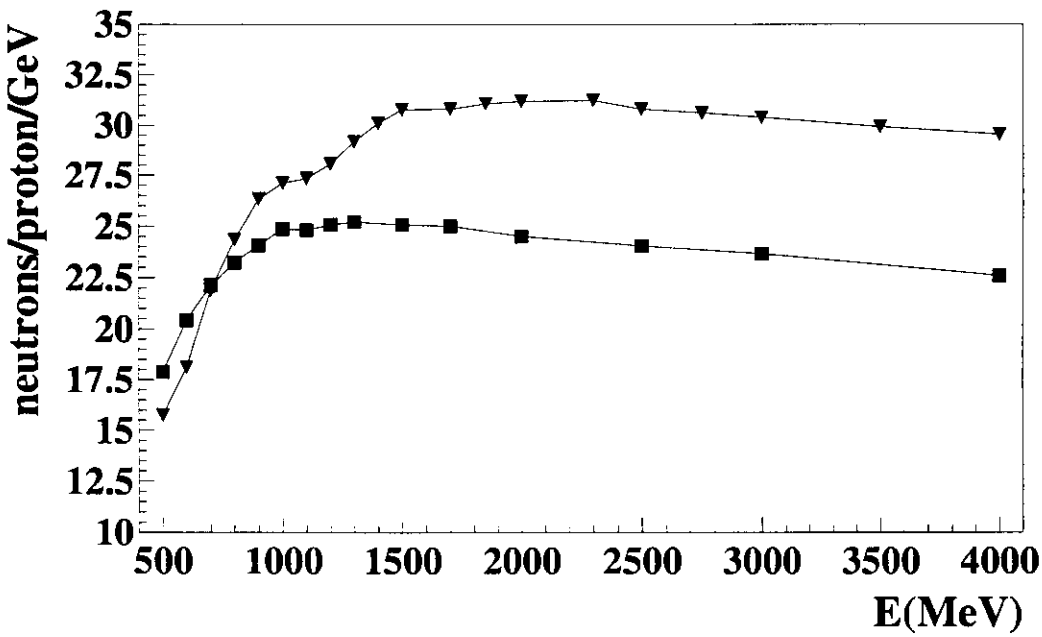

Number of low energy neutrons emitted from the lateral face of a cylindrical lead target for fixed or an optimised geometry.

Neutron energy distribution measurements
Thick target results

collaboration CEA/DSM, CEA/DAM, IN2P3

⇒ **Direct measurements of escaping neutrons**

⇒ **Test of the transport part of the simulation codes**

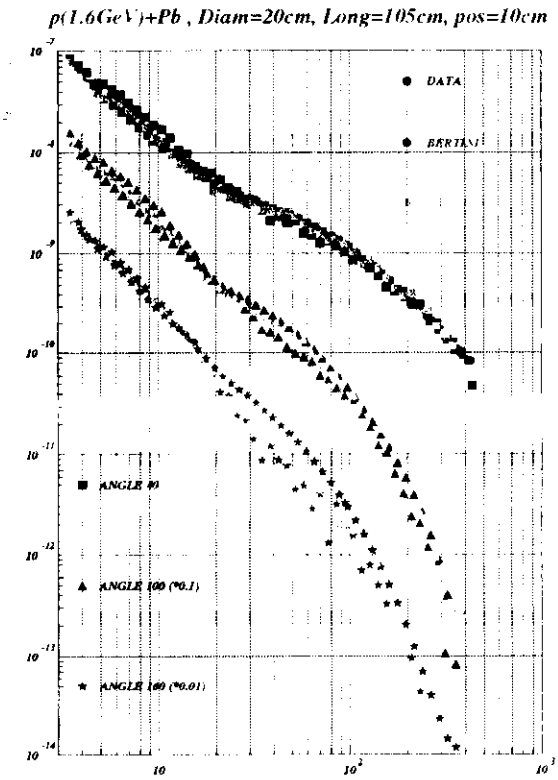

Total number of neutrons predicted by the TIERCE code :

	1200 MeV	1600 MeV
Bertini	**28.6**	**43.7**
Cugnon	**23.6**	**34.8**

p(1.6GeV)+Pb , Diam=10cm, Long=105cm, pos=10cm

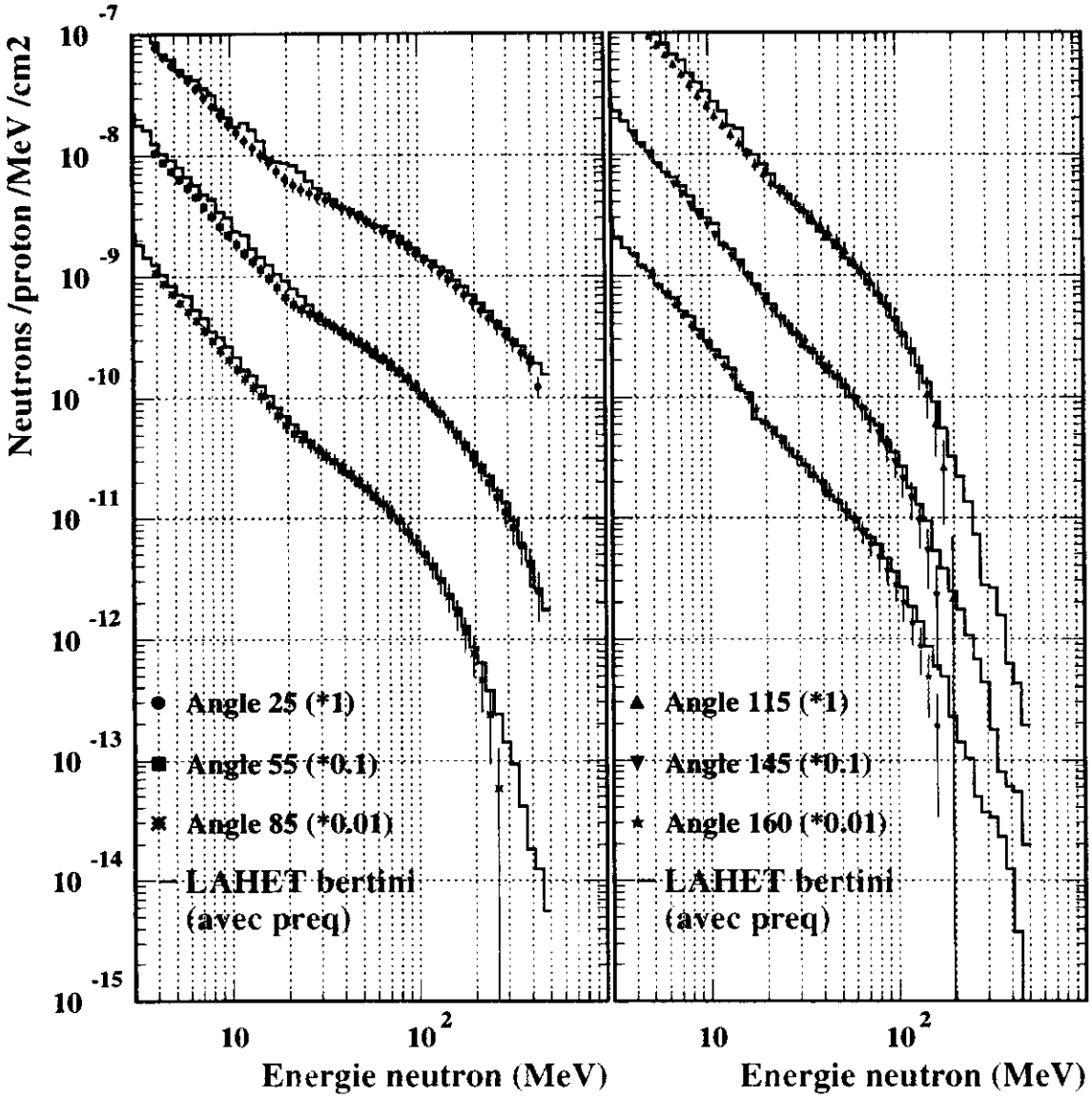

Activity in Pb and Pb/Bi targets after 1 year irradiation

E = 0.8 GeV

I = 30 mA

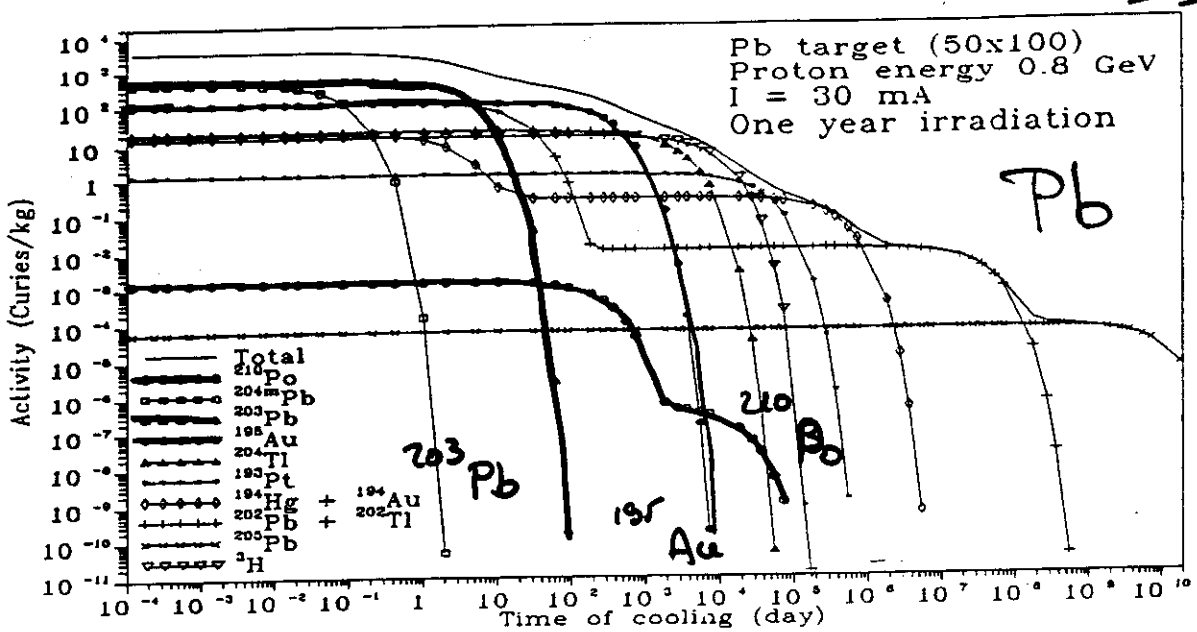

Fig. 4. Total and partial activities of lead target as a function of cooling time.

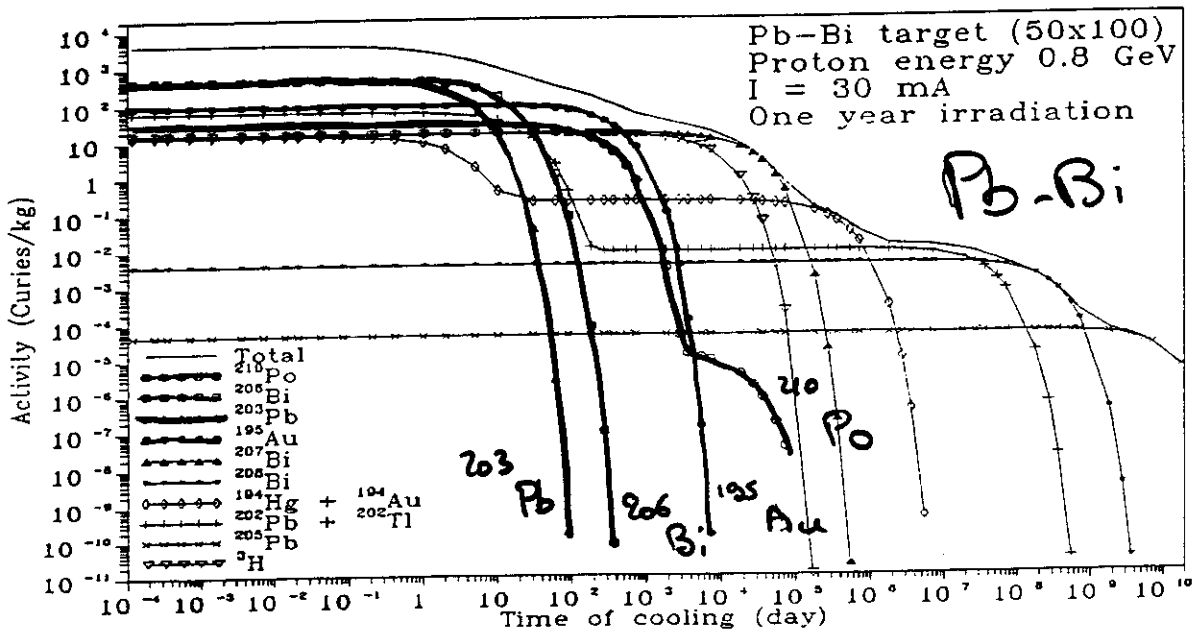

Fig. 5. The same as in Fig. 3 for lead-bismuth target.

Analysis of the Contributions of the Proton and Neutron Spectral Components to the Accumulating Activity

From Y.N. Shubin et al., Proc. ADTTA 96, Kalmar, Sweden, June 1996 p 953

Impurety production in a Fe window

Data : Webber et al., Ap. J. 508 (1998) 940
Calculation: TIERCE, p + Fe, 77 μA/cm², 573 MeV, 1 year

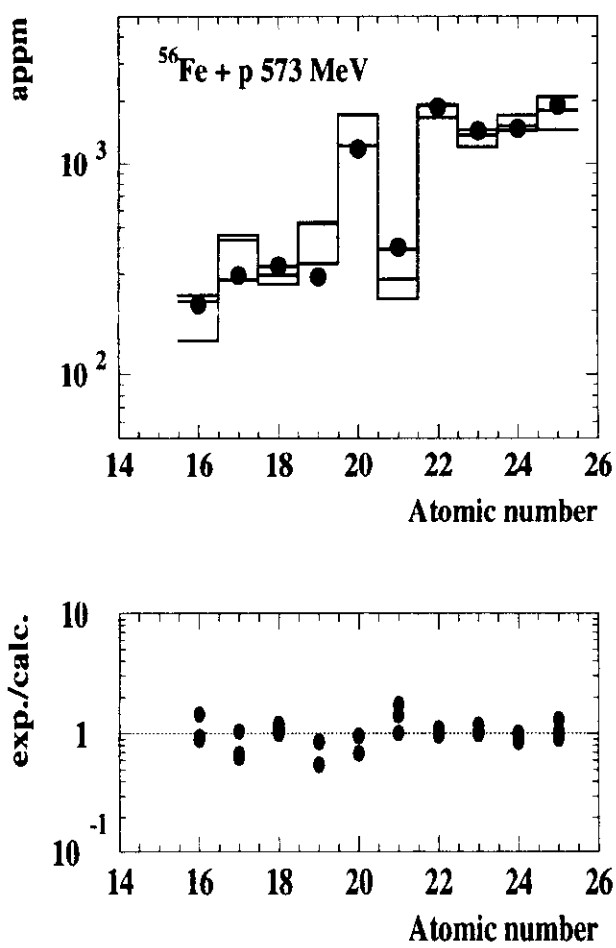

Bertini
Cugnon
Webber

➥ **Uncertainty of the order of a factor 2 in the model predictions**
➥ **Interest of parametric formulas**
➥ **Large amount of S, Ca**

II. 34

Conclusions

- **High energy nuclear data available**
  - ➥ **Neutrons: data set almost sufficient**
  - ➥ **Charged particles: data still needed**
  - ➥ **Residual nuclei: inverse kinematics data needed**
- **simulation codes**
  - ➥ **Some of the mostly used physics models clearly not suited**
  - ➥ **New models: encouraging but not yet completely satisfying**
  - ➥ **Interest of parametric formulas**
  - ➥ **Quantification of the uncertainties**
- **Perspectives**
  - ➥ **Second generation of coincidence experiments**
  - ➥ **Synthesis at European level: HINDAS**

II.35